

Aus der Klinik und Poliklinik der Nuklearmedizin
der Universität Würzburg
Direktor: Prof. Dr. med. Chr. Reiners

T-cell receptor assay and reticulocyte-micronuclei assay as
biological dosimeters for ionizing radiation in humans

Inaugural – Dissertation
zur Erlangung der Doktorwürde der
Medizinische Fakultät
der
Bayerischen Julius-Maximilians-Universität zu Würzburg
vorgelegt von
Stanislav Vershenya
aus Minsk, Weißrussland

Würzburg, Mai 2007

Referent: Prof. Dr. med. Dr. rer. nat. K. Hempel
Koreferent: Prof. Dr. med. Chr. Reiners
Dekan: Prof. Dr. med. M. Frosch

Tag der mündlichen Prüfung: 17. September 2008

Der Promovend ist Arzt

I dedicate this work to my family and thank them for all their support and love throughout all my years here, in Wuerzburg University

Contents:

1.	Introduction	1
2.	Method.....	3
2.1.	Thyroid cancer patients and radioiodine treatment (RIT).....	3
2.2.	Assays	5
2.2.1.	Standard T-Cell receptor (TCR) assay.....	5
2.2.2.	Assay for latent TCR mutants	5
2.2.2.1.	Culture of lymphocytes and detection of latent TCR mutants.....	6
2.2.2.2.	Calibration of the assay in <i>in vitro</i> irradiated lymphocytes	7
2.2.3.	MN-Tf-Ret assay	7
2.2.3.1.	Isolation of transferrin receptor positive reticulocytes (Tf-Ret).....	7
2.2.3.2.	Fixation of cells.....	8
2.2.3.3.	Flow cytometric analysis.....	8
2.3.	Irradiation and dosimetry	9
2.3.1.	Irradiation of lymphocytes	9
2.3.2.	Calculation of bone marrow radiation dose in radioiodine therapy	9
2.3.2.1.	Retrospective dosimetry according to ICRP	9
2.3.2.2.	Individual dosimetry according to MIRD	10
2.3.3.	Radiation dose due to diagnostic	12
2.4.	Statistics	12
3.	Results and Discussion	13
3.1.	Bone marrow radiation dose in RIT	13
3.2.	Standard TCR assay	14
3.2.1.	Results (standard TCR assay)	14
3.2.1.1.	TCR mutant frequency (TCR-Mf) in patients after RIT	14
3.2.1.2.	A model for the description of the course of TCR-Mf after irradiation..	18
3.2.2.	Discussion (Standard TCR Assay).....	20
3.2.2.1.	Frequency of spontaneous TCR mutants	20
3.2.2.2.	Decline of TCR-Mf and its correlation with radiation dose	20
3.2.2.3.	TCR–Mf as a biological dosimeter.....	22

3.3.	Assay for latent TCR mutants	23
3.3.1.	Results (latent TCR mutants).....	23
3.3.1.1.	Lymphocyte culture and detection of latent TCR mutants	23
3.3.1.2.	Latent TCR mutants in patients treated with radioiodine	25
3.3.2.	Discussion (latent TCR mutants)	27
3.3.2.1.	Shortening of the latent period	27
3.3.2.2.	Latent TCR mutants as a biodosimeter for recent exposure	28
3.4.	MN-Tf-Ret Assay	29
3.4.1.	Results (MN-Tf-Ret Assay)	29
3.4.1.1.	Flow cytometric measurements of micronucleated Tf-Ret.....	29
3.4.1.2.	Short time memory of MN-Tf-Ret Assay	29
3.4.1.3.	MN-Tf-Ret mutant frequency during RIT	31
3.4.1.4.	Red marrow radiation dose and f(MN-Tf-Ret)	33
3.4.2.	Discussion (MN-Tf-Ret assay)	39
3.4.2.1.	Transferrin positive reticulocytes in blood as a part of erythron.....	39
3.4.2.2.	Role of lifespan of Tf-Ret in peripheral blood	39
3.4.2.3.	Radiation dose per cycle and f(MN-Tf-Ret) in blood.....	40
3.4.2.4.	Model describing the time- and dose-dependence of f(MN-Tf-Ret).....	42
3.4.2.5.	Adaptation of the model to MN in polychromatic erythrocytes in mice.	45
3.4.2.6.	Features of the MN-Tf-Ret assay	47
3.5.	Biological dosimetry in radioiodine treated patients.....	48
4.	Summary	51
5.	References	54
6.	Abbreviations.....	63

1. Introduction

After the Chernobyl disaster the frequency of thyroid cancer has dramatically increased in children from Belarus [1-4]. The treatment for thyroid cancer is surgical removal of the tumour (thyroidectomy) followed by one or more treatments with radioiodine. In about a quarter of the Belarussian patients radioiodine therapy is performed at the Clinic for Nuclear Medicine of the University of Würzburg thanks to the financial support of the association of the German Electricity Companies (VDEW) and the 'Medizinische Hilfe für Tschernobyl-Kinder' Association.

The main risks of radioiodine treatment (RIT) are the induction of lung fibrosis and secondary cancers as a consequence of the genotoxic effects of the radioiodine radiation [5]. The frequency of somatic mutations in basic genes of erythrocytes and lymphocytes has been used as an indicator of the genotoxic effect of radiation [6-11]. The corresponding assays are 1) hypoxanthine-guanine phosphoribosyl transferase (HPRT), 2) glycophorin A (GPA), 3) T-cell receptor (TCR) assays.

In the present investigation the TCR assay was applied to the thyroid cancer patients to quantify the genotoxic effect of the radioiodine therapy and to detect those patients who might have an increased cancer risk. The patients were represented by young patients from Belarus who were undergoing the radioiodine therapy in the Clinic of Nuclear Medicine. After the irradiation with radioiodine the increase in frequency of mutant TCR receptors could be seen after a six month latent period. In order to shorten this time, for some samples the cell culture of lymphocytes had been applied before TCR assay was done.

Another method of biological dosimetry used was the reticulocyte-micronucleus assay. This method is long known and used in mice as a MN assay in polychromatic erythrocytes [12]. In humans the application of this assay was problematic because all the aberrant (in our case micronucleated) cells are quickly removed by the spleen. Therefore, in humans the assay was restricted to splenectomized subjects. Recently the flow-cytometric *in vivo* micronucleus assay

has been adapted for use in humans [13]. This is done by immunomagnetic separation of immature transferrin-positive reticulocytes (Tf-Ret) present in the peripheral blood. The isolated Tf-Ret are then analysed for the presence of micronuclei. The results of this previous study indicated that micronuclei in human Tf-Ret could be a sensitive biomarker for chromosome damage.

In order to investigate the utility and sensitivity of this method for the detection of radiation-induced chromosome damage, we have now performed a study of MN in Tf-Ret in 46 patients undergoing radioiodine therapy. These patients received defined activities of ^{131}I , precise dosimetry during their hospitalisation, and sequential determinations of the individual frequencies of MN-Tf-Ret. It was worth mentioning that this study was a first attempt of using MN-Tf-Ret assay as a biological dosimeter.

2. Method

2.1. Thyroid cancer patients and radioiodine treatment (RIT)

In most assays blood from thyroid cancer patients was used. Blood was sampled with informed consent. The thyroid cancer was caused by radioiodine incorporation around the birth or in early childhood.

The TCR assay was performed in 72 Belarusian young thyroid cancer patients, 30 males and 42 females aged between 14 and 25 years. There was no big difference in numbers of males and females, who took part in the study. Most patients were from the southern part of Belarus, which suffered heavily from the fallout of the Chernobyl accident. They had been thyroidectomised at the Republican Thyroid Cancer Centre in Minsk, Belarus before RIT in Würzburg. The data on patients at the time of thyroid cancer detection and TNM classification of the tumours are given in Tab. 1. All tumours were papillary thyroid carcinomas. Lymph nodes were involved in all patients except one. Many patients suffered from distant metastases mostly in their lungs. The unexposed control group consisted of 19 patients not yet treated with radioiodine. Their mean age was 17 years.

In MN-Tf-Ret assay 23 young women and 21 young men from Belarus and 2 elderly patients from Germany took part. The mean age of the Belarussian citizens was 19. Among them there were many patients with pathologically positive lymph nodes without (T2 N1 M0, n=23) or with metastases (T2 N1 M1, n=7). In some cases direct invasion of the tumour through the capsule of the thyroid gland was found without (T4 N1 M0, n=2) or with metastases (T4 N1 M1, n=14).

All of the patients of this study received the similar therapy. After the thyroid cancer was diagnosed the thyroid gland was surgically removed and treatment with radioiodine was started. Four weeks prior to every RIT thyroxine was withdrawn and all patients were definitely hypothyroid when radioiodine was administered as demonstrated by the high TSH level. As a consequence of hypothyroidism most patients felt tired immediately before RIT and their appetite was poor and constipation rather common. Two days after radioiodine administration thyroxine

replacement therapy was resumed by administration of about 2 µg/kg L-thyroxine and symptoms of hypothyroidism disappeared. In patients with advanced disease, several RITs were needed to cure the cancer. ¹³¹I was given orally as capsules at an activity of approximately 50 MBq per kg BW in the first RIT for ablation of remnant thyroid tissue and 100 MBq/kg in the following RITs for elimination of metastases.

Tab. 1 Thyroid cancer patients from Belarus investigated between October 2002 and June 2003 for TCR mutants

Parameter	n	%
Gender		
male	30	42
female	42	58
Age at accident (April 26, 1986)		
≤4	63	88
>4	9	12
Residence at accident		
District Gomel	28	39
District Brest	21	29
Others	23	32
Age at Diagnoses		
≤14	33	46
>14	39	54
TNM classification (papillary thyroid carcinoma)		
T1	0	0
T2	37	51
T3	0	0
T4	33	46
Tx	2	3
N0	0	0
N1	70	97
Nx	2	3
M0	26	36
M1	46	64

2.2. Assays

2.2.1. Standard T-Cell receptor (TCR) assay

The assay was performed mainly as described by Kyoizumi et al. [14]. Lymphocytes were isolated by Ficoll gradient centrifugation from a total of 6 ml heparinised blood. For flow cytometry about 5 million of lymphocytes were stained with fluorescein-labelled anti-Leu3a (CD4), phycoerythrin-labelled anti-Leu4 (CD3) antibodies (Becton Dickinson Immunocytometry Systems, San Jose, CA) and propidium iodide (PI) (20 µg/ml). The frequency of CD3+ CD4+, CD3- CD4+, CD3+ CD4- and CD3- CD4- cells was determined using a Coulter EPICS XL-MCL flow cytometer (Coulter Co, Hialeah, FI). Dead cells were excluded by the PI staining of their nuclei. TCR-Mf was the number of CD4+ CD3- cells divided by the total number of CD4+ cells. Every lymphocyte fraction was analysed twice and then the mean value was taken. Flow cytometric analysis and gating of lymphocytes are described in results.

2.2.2. Assay for latent TCR mutants

TCR assay for latent TCR mutants was done in parallel with standard TCR assay. So we used the same blood samples for both of them. All these patients were from Belarus. Their characteristics were as described above. We investigated 26 of them, 18 females and 8 males, aged between 13 and 19 with mean value of 18 years. For the assay it was important to separate the first time-treated patients from those treated 2 and more times.

Tab. 2 Number of treatments with radioiodine

Number of RIT	Number of Patients
1	8
2	13
3	2
4	1
5	1
6	1
Totally: 26 patients	

2.2.2.1. Culture of lymphocytes and detection of latent TCR mutants

In these patients blood was taken before and 96 hours after the RI (radioiodine) application. All the blood was taken in heparinised tubes. The blood taken before the RIT (18 ml) was divided into 3 samples. 1st blood sample was used for standard TCR assay as described above.

In 2nd and 3rd samples, as well as in the probe taken 96 hours after the start of treatment, the lymphocytes were isolated by ficoll gradient centrifugation and then washed twice in RPMI1640 by centrifugation (at +4°C, 1100 RPM, 30 min, without brake). Lymphocytes from the 3rd sample were irradiated with 1Gy before the cell culture (Section 2.3.1).

The amount of $4.6 \cdot 10^6$ cells was taken and placed in 23 ml of culture medium at 37°C, 5% CO₂. The starting concentration was $0.2 \cdot 10^6$ cells per 1ml. The culture medium compounds are summarised in Tab. 3 [15]. Six days later the TCR assay was performed. When lymphocytes were cultured for more than 6 days, half the culture medium was replaced every 2 days.

For the assay 5 to 10 ml culture medium were taken, cells were separated by pipetting, counted and washed twice with PBS. Finally, the pellet was suspended in 100 µl and cells were stained as usual for TCR assay. The overall cell concentration was calculated by multiplying the actual concentration in the solution by the dilution coefficient.

Tab. 3 Lymphocyte cell culture medium

Name of Compound	Amount
RPMI1640 medium (Dutch modification) with 15% FBS	80 ml
AIM-V medium	20 ml
Penicillin-Streptomycin solution (conc.: Penicillin - 10000 E/ml, Streptomycin – 10000 ug/ml)	2 ml
Sodium-Pyruvat stock solution (100 mM)	1 ml
Glutamax I stock solution (200 mM)	1 ml
Mercaptoethanol stock solution (50 mM)	100 µl
Phytohemagglutinin stock solution (3 µg/ml)	300 µl
Rec-IL-2 stock solution (400000 U/ml)	50 µl

2.2.2.2. Calibration of the assay in *in vitro* irradiated lymphocytes

Additionally, for TCR assay after *in vitro* culture and irradiation, we performed the calibration test to check the TCR-Mf response to different levels of *in vitro* irradiation. The procedure was the same as described above for sample 3, except that the blood was taken from a healthy volunteer with normal TCR-Mf base level and afterwards, it was divided into 6 samples, which were irradiated at doses from 0 to 1 Gy with a 0.2 Gy step as described in Section 2.3.1.

2.2.3. MN-Tf-Ret assay

2.2.3.1. Isolation of transferrin receptor positive reticulocytes (Tf-Ret)

Coating of Dynabeads. 45 μ l magnetic beads (CELLlection™ Pan Mouse IgG Kit, Dynal, Oslo) were transferred to a conical tube. The tube was placed in a magnetic particle concentrator (MPC) for 1 minute. The liquid was removed and the beads were resuspended in 2 ml phosphate buffered saline pH 7.4 (PBS) with 1% foetal calf serum (FCS). The tube was placed in the MPC for one minute and the liquid was taken away. The wash with PBS containing 1% FCS was repeated.. The beads were then resuspended in 100 μ l PBS with 1% FCS and 7 μ l mouse anti-human CD71 antibody was added. The tube was incubated for 30 minutes at room temperature with continuous rotation. During this time the CD71 antibody was attached to the magnetic beads. After the incubation 2 ml PBS with 1% FCS was added and the tube was placed in the MPC for 1 minute. The liquid was removed and the bead-antibody complex was washed two more times with 2 ml PBS containing 1% FCS and finally suspended in 100 μ l PBS with 1% FCS.

Isolation of Tf-Ret. Whole blood samples were taken by vein puncture. To remove the serum containing free transferrin receptors, 2 ml whole blood was placed in a tube together with 4 ml PBS (without FCS) and centrifuged at 400 \times g for 5 min at room temperature. The pellet was washed again in 4 ml PBS and centrifuged as before. The pellet was resuspended in 0.5 ml PBS. Then the blood cells were added to the tube with the bead-antibody complex. The tube was

incubated at 4°C for 15 minutes with continuous rotation. This incubation allowed the cells with CD71 on their surfaces to attach to the bead-antibody complex. Thereafter the tube was placed in the MPC for 1 minute. The liquid was removed. The magnetically labelled cells were washed four times with 3 ml PBS containing 1% FCS. Before the last wash the suspension was transferred to a new conical tube. The magnetically labelled cells were resuspended in 200 µl PBS with 1% FCS and 7 µl DNase from the CELLection™ Pan Mouse IgG Kit was added. The tube was incubated for 15 minutes at room temperature with continuous rotation.

During this step DNase released the cells from the beads due to enzymatic cleavage of the DNA-linker. The tube was then placed in the MPC for 1 minute. The fluid was collected into a new conical tube. The beads were washed with 200 µl PBS containing 1% FCS four times and the fluid was collected into the tube with the released cells (final volume of 1 ml). Before the last wash the suspension was transferred to a new conical tube and the tube with the released cells was placed in MPC once more to remove residual beads. The cell suspension was collected to a new tube again.

2.2.3.2. Fixation of cells

The tube with the reticulocytes was centrifuged at 400×g for 5 min at room temperature. The supernatant was discarded and the pellet was resuspended in 0.4 ml PBS with 10 µg/ml SDS. After one minute 2.5 ml 2% formaldehyde with 10 µg/ml SDS was added during mixing. The tube was stored in a dark place at room temperature for at least three days.

2.2.3.3. Flow cytometric analysis

Staining of cells: the tube with the cells was centrifuged at 400×g for 5 minutes at room temperature. The pellet was resuspended in 0.5 ml staining solution [prepared by mixing 10 ml PBS with 7.5 µl Hoechst 33342 stock solution (500mM) and 2 µl Thiazole orange (1 mg/ml)]. The tube was incubated at 37°C for 60 minutes. The tube was mixed every 20 minutes.

Flow cytometry: The stained samples (whole blood and enriched reticulocytes) were analysed on a LSR flow cytometer (Becton-Dickinson, CA, USA) equipped with an argon ion laser operating at 488nm and a second HeCd ion laser operating at the 352 nm. The analysis rate was 300-1000 cells per second with a threshold in forward scatter (FSC) set to include all intact cells. Using CellQuest Pro software (Becton Dickinson, CA, USA) peak values for FSC, SSC, Thiazole orange fluorescence and Hoechst 33342 fluorescence signals were collected. The FSC signals were acquired using a linear scale and the SSC, Thiazole orange and Hoechst 33342 signals were acquired using a log scale. Between 100.000 and 200.000 events were collected from each sample.

2.3. Irradiation and dosimetry

2.3.1. Irradiation of lymphocytes

Lymphocytes were placed in 1 ml of ice-cold culture medium RPMI1640 in cryotubes and irradiated at dose 1 Gy, dose rate 1,62 Gy/min, with 0.66 MeV Photons from a calibrated ^{137}Cs -source.

2.3.2. Calculation of bone marrow radiation dose in radioiodine therapy

In the case of MN assay for every patient individual dosimetry was done as described below. For TCR assay dosimetry on individual basis wasn't possible, therefore, the retrospective dosimetry was done. Obviously, the retrospective dosimetry is less accurate and some mistakes inevitably occur.

2.3.2.1. Retrospective dosimetry according to ICRP

Dose determination is related to red marrow as central organ of hematopoiesis. The red marrow dose of radioiodine treated patients was calculated by the Eq. 1, where D is the total dose (mGy) in the red marrow, RM - the marrow dose per unit of activity administered (mGy/MBq), and A - total activity given. The value for RM was taken from pamphlet 53 [16] of ICRP (International Commission on Radiological Protection) using the data of the appropriate phantom. In ICRP

pamphlet all the coefficients are calculated for a person with a 70 kg weight, or a phantom. In our equation we took into account the actual difference between the patients-weight and phantom-weight, and represented it as additional coefficient. The factor 1.45 (SD = 0.29) accounts for the fact that the excretion of iodide ions in thyroidectomised and hypothyroid patients is much slower than assumed by ICRP for healthy individuals. Its value was found in an investigation with 22 young thyroid cancer patients (12 men and 10 women) [17], whose red marrow dose was calculated according to ICRP as well as measured as recommended by Medical Internal Radiation Dose (MIRD) Committee [18, 19].

$$D = 1.45 \times RM \times A \times \frac{\text{Phantom} - \text{Weight}}{\text{Patient} - \text{Weight}} \quad \text{Eq. 1}$$

2.3.2.2. Individual dosimetry according to MIRD

Dosimetry is restricted on red marrow (RM) since this is the critical organ in MN-Tf-Ret biodosimetry. The following parameters were measured to calculate the dose to RM: a) the administered ^{131}I activity A_0 and b) the cumulated total body activity A_{TB} . The latter was determined by sequential measuring of the total body activity (TB_{act}) with a calibrated survey meter nominally at 2 h, 4 h, 6 h, 12 h, 24 h, 36 h, 48 h, 72 h, and 96 h after ^{131}I administration. The initial whole body quantitation at 2h post-administration was performed with no interim voiding, allowing patient specific standardization of the survey meter. The area under the total activity curve is equal to A_{TB} . In calculation of the cumulated total body activity it was assumed that the decay from the last data point corresponds to the decay within the last 2 days. In some patients TB_{act} could not be measured for 96 hours, since they left the hospital as soon as TB_{act} fell to less than 250 MBq. This value was the lower limit of TB_{act} when patients had to stay in the hospital according to German regulations.

$$D_{RM} = A_{RM} \times S(RM \leftarrow RM) + A_{RB} \times S(RM \leftarrow RB) \quad \text{Eq. 2}$$

Red marrow dose estimates were calculated by the two component Eq. 2 [20], where D_{RM} is the red marrow dose estimate, A_{RM} is the red marrow cumulated activity, $S(RM \leftarrow RM)$ is the red marrow-to-red marrow S value, A_{RB} is the remainder of the body (RB) cumulated activity obtained by subtracting the red marrow value, A_{RM} , from the total body value, and $S(RM \leftarrow RB)$ is the remainder of the body-to-red marrow S value. S values were taken from MIRDOSE3 [18]. MIRDOSE3 assumes homogenous activity distribution throughout RB. As in bone components (i.e. trabecular and cortical bone) activity would be much lower than in other organs, bone was considered as a source region with zero residence time to avoid false cross-fire of electrons from bone to RM [19].

$$A_{RM} = [A]_{blood} \times m_{RM, model} \times \frac{m_{TB, patient}}{m_{TB, model}} \times CF \quad \text{Eq. 3}$$

The red marrow cumulated activity, A_{RM} , in Eq. 2 was determined by Eq. 3, where $[A]_{blood}$ is the cumulated activity per 1 liter blood, $m_{RM, model}$ is the red marrow mass of the respective dosimetric model, $m_{TB, patient}$ is total body mass of the patient, $m_{TB, model}$ is the total body mass of the respective model. CF is a correction factor for the marrow-to-blood activity concentration ratio. CF was set at unity under the assumption that iodide distributes equally between the water pool of blood and red marrow. In RIT of thyroidectomised patients ^{131}I activity is present in the form of iodide. $[A]_{blood}$ was not measured in the present investigation. It was calculated by the equation $[A]_{blood} = f \times A_{TB} / V_{blood}$ where f is a constant factor which corresponds to the cumulated activity ratio A_{blood} / A_{TB} [21, 22]. The value of f is 0.123 ± 0.015 (mean \pm SD). It was found by an investigation in 22 young adults whose cumulated total body activity as well as the cumulated blood activity

had been measured during RIT for thyroid cancer [17]. V_{blood} is the patient's blood volume, which was calculated considering the patient's gender, weight and height [23]. Some details about the treatment and radiation dose to red marrow are given in Tab. 4

2.3.3. Radiation dose due to diagnostic

Some hours before ^{131}I administration every patient was screened for lung metastases by a CT examination of the chest (spiral CT scanner Somatom Plus 4A, Siemens AG, Forchheim, Germany). The radiation dose applied by the CT scan is about 15 mSv to the red marrow of the thorax [24]. Bones of the thorax (sternum, ribs, scapulae, clavicles, and upper fourth of the humeri) contains in adult about 20 % of total red marrow [25]. The dose of diagnostic radiology was not considered. It should be less than 5% of the dose from radioiodine administration.

2.4. Statistics

For non-linear regression analysis the software SigmaStat 1.0 (Jandel Scientific, Erkrath, Germany) was applied, which uses the Marquardt-Levenberg algorithm to find the parameters of the variables that give the best fit.

3. Results and Discussion

3.1. Bone marrow radiation dose in RIT

Some details about the treatment and the radiation dose to red marrow are given in Tab.4. In the first RIT about 50 MBq and second RIT about 100 MBq per kg BW were administered. Patients were exposed to an exponential decreasing low dose rate irradiation of β - and γ -rays for 3 to 6 days. In the first day after radioiodine administration, the dose rate was in the order of 5-10 mSv/h. The mean total radiation dose to red marrow (D_{RM}) was 182 and 475 mSv in the first and

Tab. 4 Radioiodine therapy and radiation dose to red marrow

No. of RIT	^{131}I Act. (MBq / kg)	Age (a)	BW (kg)	Pause a (y)	TSH b (mU / L)	τ_{TB} c (h)	D_{24} e (mSv)	D_{RM} d (mSv)
1st (17) f	50	17.7 \pm 1.7 (13.0 - 19.7)	61 \pm 12 (40 - 80)	--	190 \pm 119 (14 - 431)	16.9 \pm 3.1 (11.9 - 21.8)	137 \pm 16 (95 - 153)	182 \pm 32 (112 - 223)
2nd (17) f	100	18.1 \pm 1.3 (14.5 - 19.8)	64 \pm 10 (42 - 82)	0.8 \pm 0.1 (0.5 - 1.0)	253 \pm 194 (56 - 688)	21.7 \pm 4.7 (14.6 - 32.7)	313 \pm 41 (236 - 378)	475 \pm 112 (309 - 727)
3rd - 12th (15) f	100	18.8 \pm 1.8 (17.0 - 24.5)	70 \pm 13 (47 - 91)	1.6 \pm 1.3 (0.8 - 5.7)	283 \pm 132 (104 - 633)	18.3 \pm 2.4 (14.4 - 22.3)	289 \pm 27 (250 - 332)	398 \pm 60 (308 - 484)

- a Time interval between the present and previous RIT.
b Concentration of thyroid stimulating hormone (TSH) in plasma, value in healthy persons 0.3 – 4 mU/L
c Residence time (RT) of radioiodine in total body (TB). It was calculated by the equation $\tau_{TB} = A_{TB} / A_0$ where A_{TB} is cumulated total body activity and A_0 is the administered activity.
d Radiation dose to red marrow, for details see 2.3.2; values are corrected for the indicated activity.
e Radiation dose during the first 24 h after ^{131}I administration. It was calculated by the relation $D_{24} \approx D_{RM} \times (1 - \exp(-24 / \tau_{TB}))$. D_{24} is the greatest radiation dose per cell cycle in late erythroblasts, for details see 4.2
f Only patients below age 25 at RIT

second RIT, respectively. Though in each group about the same activity per kg BW was administered the red marrow dose scattered in a wide range in consequence of the considerable variation of the total body residence time (τ) of radioiodine. The red marrow doses in our patients were in the same range as previously reported, if the differences and uncertainties in dose calculation are considered [22, 26, 27]. Besides, the total red marrow dose D_{RM} also the dose during the first 24 h of RIT (D_{24}) is given. In the present study, the dose ratio D_{24} / D_{RM} varied between 0.47 and 0.86 (median 0.72). It will be shown in Section 3.4.2.4 that the knowledge of D_{24} is a prerequisite for the understanding of the time curve of f(MN-Tf-Ret) in patients after RIT.

3.2. Standard TCR assay

3.2.1. Results (standard TCR assay)

3.2.1.1. TCR mutant frequency (TCR-Mf) in patients after RIT

Fig. 1 represents examples flow of cytometric analysis of TCR mutants in a healthy person and in a patient treated several times with radioiodine. The mutant window used in the present investigation is as described by Kyoizumi et al. [14]. In their analysis the mutant window was set to the region where the CD3 level (FL2) was <4% of that of normal CD4+ cells. The left and right limits of FL1 were set at values half of and two times greater than the mode intensity of FL1 for normal CD4 T-cells. The mean TCR-Mf of patients before ^{131}I treatment, the so-called spontaneous mutant frequency, was $2.0 \pm 0.6 \times 10^{-4}$ (mean \pm SD, n=25). TCR-Mf of the radioiodine treated patient was significantly higher than that of the untreated one.

In Tab. 5 the results of all TCR assays in radioiodine treated young patients are summarized. As it could be seen from the table, even more than 10 years after the last treatment TCR-Mf has not yet returned to normal.

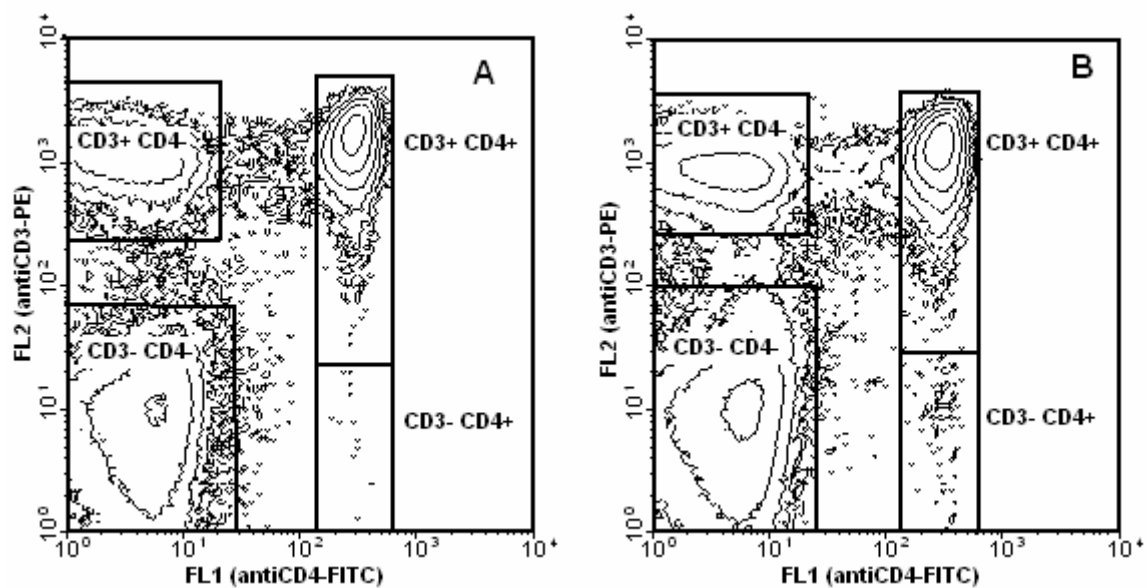


Fig. 1 Flow cytometric analysis of TCR mutant lymphocytes.

A. Healthy donor with normal level of TCR-Mf 1.73×10^{-4} .

B. Sample of a patient treated with radioiodine 8 times between 1994 to 1999 with cumulated activity of 47GBq, TCR-Mf 4.89×10^{-4} . The gating of TCR mutants is described in text.

Tab. 5 Time table of ¹³¹I treatment and TCR-Mf in treated patients from Belarus

Patient \ Years	0	1	2	3	4	5	6	7	8	9	10	11	12
W240	1.6 *												
W241	2.8 *												
W242	2.4 *												
W243	1.8 *												
W244	1.5 *												
W245	1.6 *												
W222	* 1.9												
W226	1.7 *												
W229	1.7 * 2.4 *												
W230	1.8 * 4.3 *												
W231	1.9 * 2.6 *												
W232	2.2 * 4.4 *												
W233	1.8 * 1.8 *												
W234	2.6 * 3.9 *												
W235	2.8 * 4.2 *												
W236	1.8 * 4.1 *												
W237	1.2 * 3.6 *												
W238	1.3 * 4.4 *												
W239	3.3 * 4.6 *												
W223	1.3 * 1.4 *												
W224	1.7 * 2.2 *												
W227	2.0 * 4.2 *												
W214	*	2.9 *											
W215	* 2.8 *	3.0											
W216	*	2.2											
W219	* 2.1 *	4.0 *											
W220	1.5 *	2.8 *											
W221	3.3 * 2.5 *	5.4* 8.5 *											
W225	2.5 * 3.3 *	6.9 *											
W228	1.6 *	2.5 *											
W190	**	**	4.4										
W207	**	*	10.2 *										
W187	***	*	*	11.9									
W204	**	**		8.4									
W206	***	*	5.9 *	10.2									
W211	**		6.1	7.3 *									
W212	**	*	6.2 *	6.6									
W218	**	**	*	12.0									

Tab. 5 Time table of ^{131}I treatment and *TCR-Mf* in treated patients from Belarus (continued)

Patient \ Years	0	1	2	3	4	5	6	7	8	9	10	11	12
W170	***	*	**	7.0	11.0								
W174	***			4.2	2.9								
W176	**	**	*	5.9	7.5								
W183	**	*	3.4 *	6.0	7.3								
W195	***	*		8.4 *	7.8 *								
W197	**		* 8.0		7.4								
W141	***	*	**		4.6	4.6							
W092	***	**		*	*		3.8						
W117	**	*	*				3.1 *						
W119	***					4.0	4.5						
W135	**	*	*				7.4						
W013	***	**	*					3.9					
W018	***	***	*	*			4.4	3.6					
W058	***	**	*	*	*			8.3					
W093	***	*	*					4.0					
W005	***	**							4.3				
W014	***	**		*					5.3				
W065	**	*							3.8				
W009	***	**	*		*					5.8			
W011	***	***	*	*	*		*		7.5	5.8			
W024	***	**	*	*						6.7			
W047	***	**	*	*			*			3.5			
W053	***	**								2.6			
W010	***	**	*	*			*	*		9.5 *	6.6		
W035	***	***	**								5.0		
W038	***	**	**	*							2.9		
W051	***	**	*	*		*			4.7 *	4.3			
W054	***									2.3			
W055	***	**								2.8			
W180	*					**	**	*	*	12.2 *	11.8		
W036	**	**	*	***	*								2.5
W037	***	**	**	**	*								3.0
W042	***	*		***	**	*							4.2
W091	***				**	*	*	*	*			7.7 *	7.7

Every number represents the value of TCR-Mf times 10^{-4} . Stars (*) represent a treatment. Years indicate the number of years passed since the 1st treatment.

For example '1.5 * 2.8 *' (patient W220) means that Mf at start, or base level, was 1.5×10^{-4} . Right after the TCR assay the patient received his 1st treatment. The next year he came to the clinic again, and Mf was measured once more, followed by second treatment. Initially the level of Mf increases as a consequence of the repeated radioiodine therapies but later on Mf goes down due to the elimination of mutants from the organism.

3.2.1.2. A model for the description of the course of TCR-Mf after irradiation

The Mf decay in years following RIT can be described by the three parameter single exponential decline function Eq. 4,

$$Mf = Mf_0 + k \times D \times e^{-b(T-0,5)} \quad \text{Eq. 4}$$

$$Mf = Mf_0 + \sum_{n=1}^i k \times D_i \times e^{-b(T_i-0,5)} \quad \text{Eq. 5}$$

where Mf_0 is the spontaneous mutant frequency, k - a coefficient showing the increase in Mf per 1 mGy radiation dose to red marrow, D – the total dose in mGy per treatment, and b – the elimination coefficient of mutants. Its dimension is year⁻¹ and it corresponds to the reciprocal mean residence time of TCR mutants. T is the time between measurement of Mf and the treatment in years. The value -0.5 considers the fact that the maximum of Mf is reached not before a period of about half a year. Since most of the patients were treated with radioiodine more than once, the level of Mf is described by the sum of i exponential decay functions (Eq. 5), where i corresponds to the number of treatments. In the present cohort of patients the highest number of treatments was ten.

Our goal was to find the values for the coefficients Mf_0 , k and b, which fit best to the measured mutant frequencies in Tab. 5, where the absorbed dose for every treatment (D_i), and the time between treatment and the measurement (T_i) were known. The values of these coefficients are given in Tab. 6. They were found by nonlinear regression analysis of Eq. 5 using the software SigmaStat 1.0. The correlation between calculated Mf values and measured values was satisfactory (Fig. 2).

Tab. 6 Values of the parameters of Eq. 4 and 5

Parameter	Value	SE	CV (%)	Dimension
Mf_0	2.0×10^{-4}	3.3×10^{-5}	15.6	
k	6.5×10^{-7}	10.5×10^{-8}	12.1	mGy ⁻¹
b	2.5×10^{-1}	3.4×10^{-2}	15.6	year ⁻¹

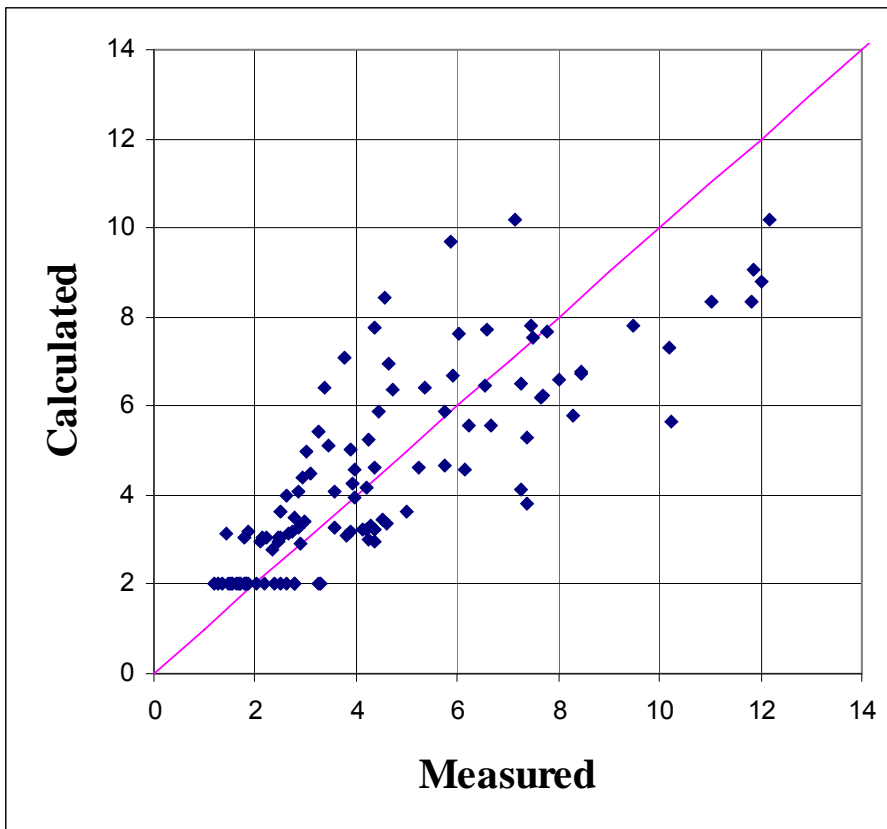


Fig. 2 The correlation between the measured and calculated values of TCR-Mf.

None of our patients had the TCR-Mf level deviating considerably from the regression curve. If calculated value was significantly lower than measured one, this could indicate a higher radiosensitivity of the respective patient.

3.2.2. Discussion (Standard TCR Assay)

Some essential parameters of the standard TCR assay are summarised in Tab.7. Data were taken or calculated from data in Tab. 6.

Tab. 7 Parameters of the standard TCR Assay

Parameter	Value*
Spontaneous TCR-Mf	2.0×10^{-4}
Half life	2.8 years
Doubling Dose	308 mGy

* Data taken or calculated from data in Tab. 6, column 2

3.2.2.1. Frequency of spontaneous TCR mutants

The value of Mf_0 in Tab. 7 partly supports the results of previous investigations [28], where the age dependency of TCR-Mf is given by the equation $Mf_0 = (1.9 + 0.02 \times age) \times 10^{-4}$. According to this equation, Mf_0 of a 17 year old patient would be 2.24×10^{-4} . The half-life of TCR mutants in peripheral blood was 2.8 years.

3.2.2.2. Decline of TCR-Mf and its correlation with radiation dose

As a consequence of this slow decay of TCR-Mf, a radiation induced increase of Mf will not return to normal before 5 to 15 years (Fig. 3). In patients after RIT [4] as well as in gynaecological cancer patients after radiotherapy [29], a slightly shorter half-life of mutant T-cells (2 to 3 years) was found. It is worth mentioning that T lymphocytes with radiation-induced unstable chromosome damage, which die in their first mitosis, could be detected more than ten years after exposure [30].

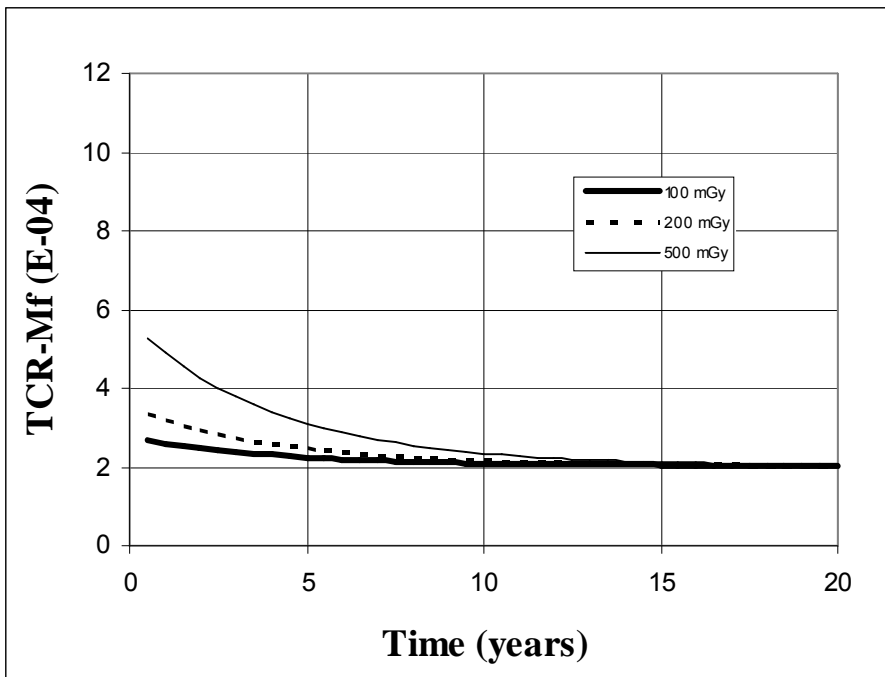


Fig. 3 Increased TCR-Mf after irradiation and its exponential decay to normal level over time. Curves were calculated by Eq. 4 using the values of Tab. 7.

The parameter k gives the increase in TCR-Mf per 1 mGy radiation dose to red marrow. Their value are $6.5 \times 10^{-7} \text{ mGy}^{-1}$. Akiyama et al. [7] had measured the increase in TCR-Mf in radioiodine treated patients as a function of the ^{131}I activity administered. They found that Mf increased by 6×10^{-5} per 1 GBq administered activity. If we assume a body weight of approx 70 kg, this activity would result in a red marrow dose of approx. 50 mGy (Eq. 1). The corresponding value of k is $12 \times 10^{-7} \text{ mGy}^{-1}$. This is approximately 2 times higher than that of our young patients.

3.2.2.3. TCR–Mf as a biological dosimeter

If there was only one treatment with radioiodine or one X-ray exposure, TCR-Mf might be used as a biological dosimeter, since the relationship between the radiation dose and the maximum of Mf is given by the Eq. 6 as demonstrated in Fig. 4. Eq. 6 derives from Eq. 4, if the exponent becomes zero. The radiation doses, which doubles TCR-Mf is 310 mGy. Naturally, this calibration curve can only be used if the quality of the radiation, the dose-rate, and the dose range are comparable with the conditions in radioiodine therapy.

$$Mf_{MAX} = 2.03 \times 10^{-4} + 6.5 \times 10^{-7} \times D \quad \text{Eq. 6}$$

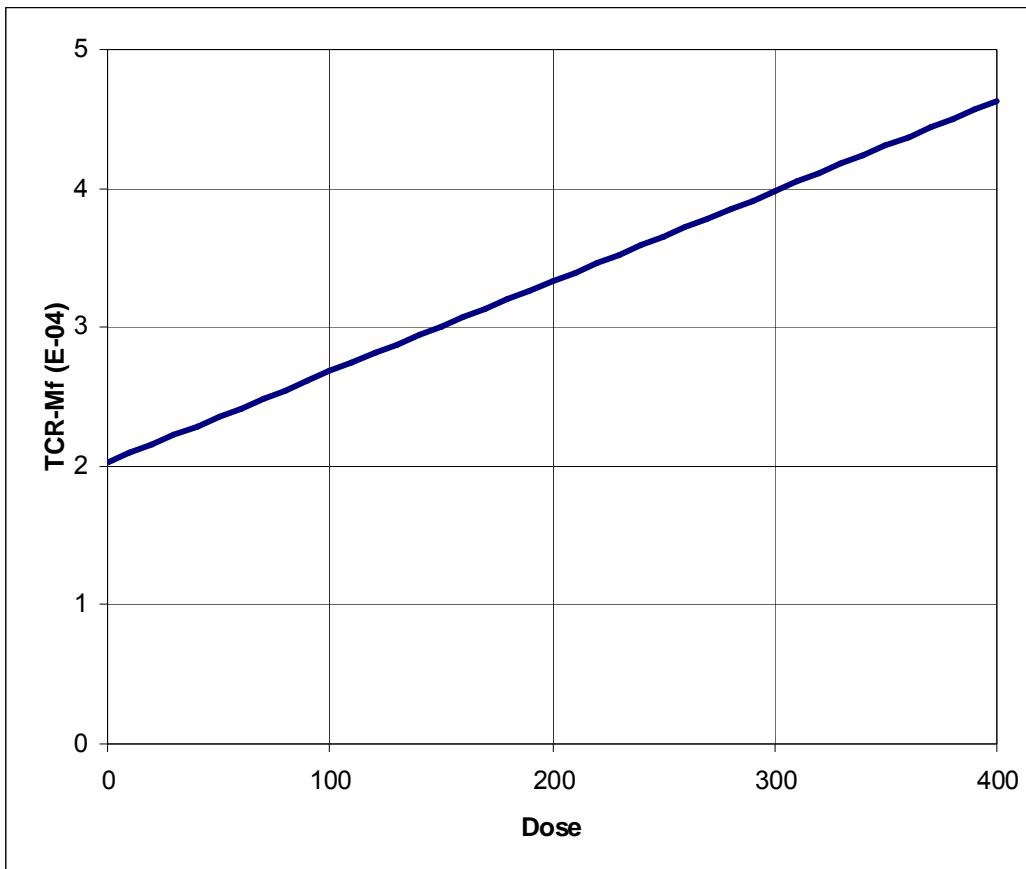


Fig. 4 TCR-Mf as a function of radiation dose to red marrow half a year after exposure

3.3. Assay for latent TCR mutants

A disadvantage of the TCR assay as a biological dosimeter is that it cannot be used before about half a year after exposure. This disadvantage might be overcome by *in vitro* incubation of lymphocytes shortly after their irradiation as shown by Ishioka et al. [31].

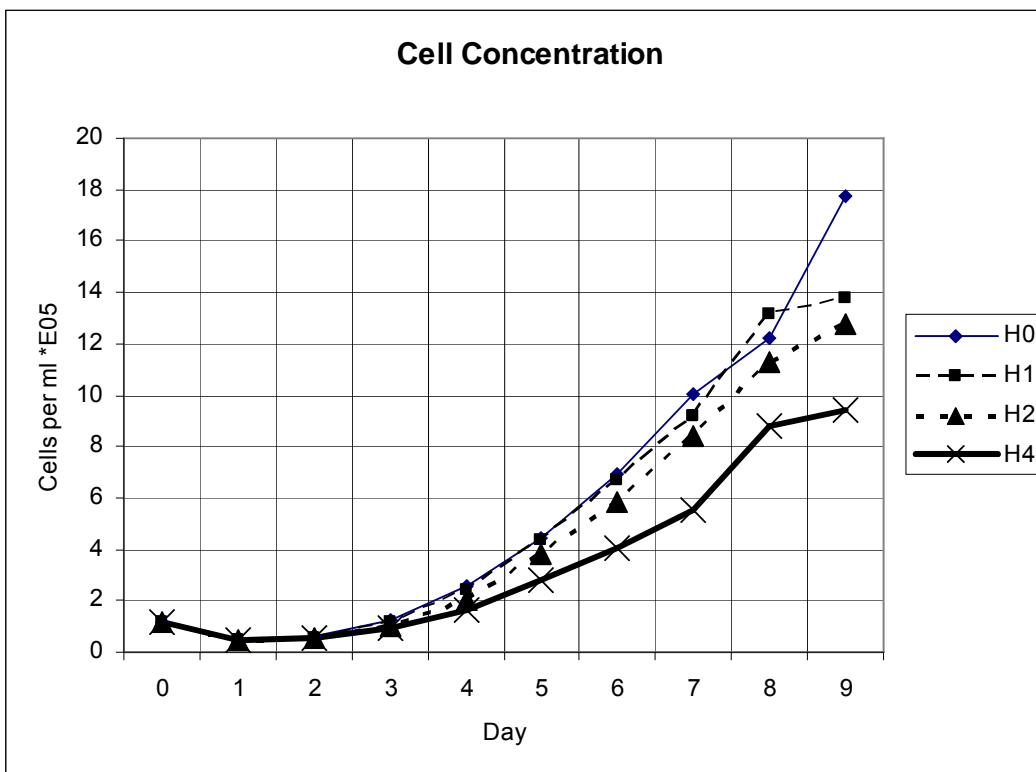


Fig. 5 Proliferation of irradiated lymphocytes *in vitro*.

H0 – non-irradiated control, H1 – irradiated with 1 Gy, H2 – irradiated with 2 Gy, H4 – irradiated with 4 Gy

3.3.1. Results (latent TCR mutants)

3.3.1.1. Lymphocyte culture and detection of latent TCR mutants

During this experiment 1) a protocol for the *in vitro* culture of irradiated lymphocytes was optimised (Fig. 5 and Fig. 6), 2) calibration curves of TCR-Mf *in vitro* irradiated lymphocytes were established (Fig. 7), and 3) the standard protocol

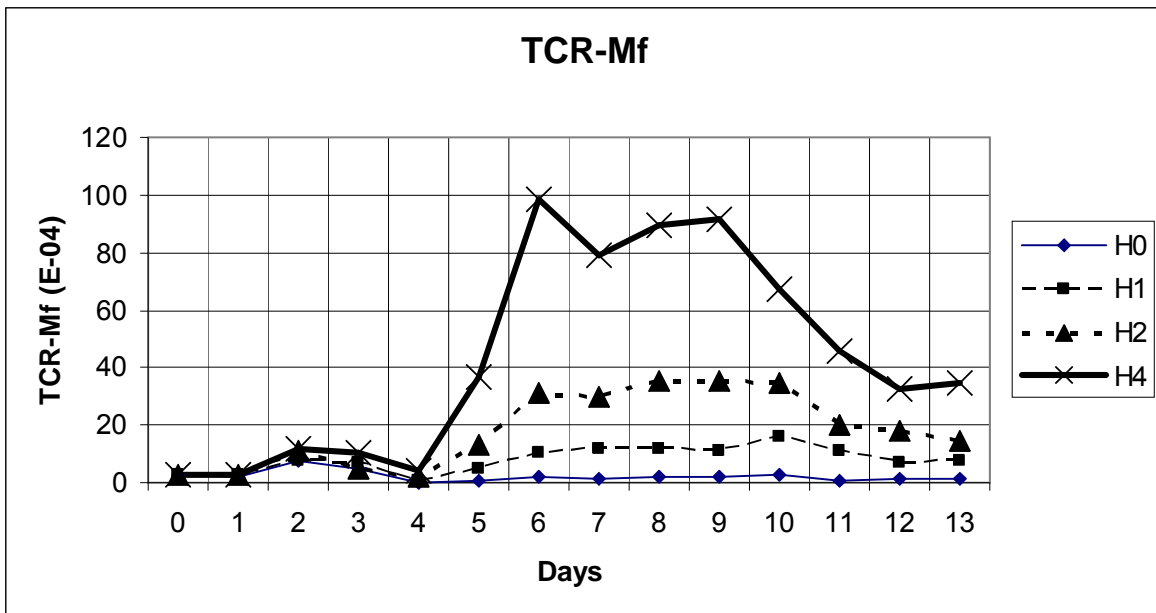


Fig. 6 TCR-Mf of irradiated lymphocytes during proliferation in culture.

H0 – unirradiated control, H1 – irradiated with 1 Gy, H2 – irradiated with 2 Gy, H4 – irradiated with 4 Gy

for detection of latent TCR mutants was established and tested on patients after RIT. At the beginning we wanted to find out the rate of lymphocyte growth and profile of TCR-Mf depending on the day of incubation and dose of external irradiation. For these purposes blood samples from the same person were irradiated *in vitro* with 1 Gy, 2 Gy and 4 Gy and incubated. The starting concentration of cells in the medium was $1 \cdot 10^5$ cells/ml. Also, the medium was diluted throughout the incubation, as soon as the concentration of lymphocytes exceeded 10^6 cells/ml, to prevent the high cells concentration, which would arrest cell divisions. Irradiation procedure was described in “Methods” (Section 2.2.2.1).

The cell concentration and TCR-Mf were measured every day and the results could be seen in the Fig. 5 and 6. It is worth mentioning that on day 1 the concentration of lymphocytes was dropping from $1.2 \cdot 10^5$ to $0.5 \cdot 10^5$, and not until after 2 days in culture would they start to proliferate. The Mf reaches its maximum on day 6 of incubation with clear dependence on the irradiation dose. On day 9 the mutant lymphocytes (lacking CD3 receptor) are overgrown by normal lymphocytes and the Mf goes down. Therefore, TCR assay with incubated lymphocytes was also performed on day 6 of the incubation, so the maximum of TCR-Mf could be seen.

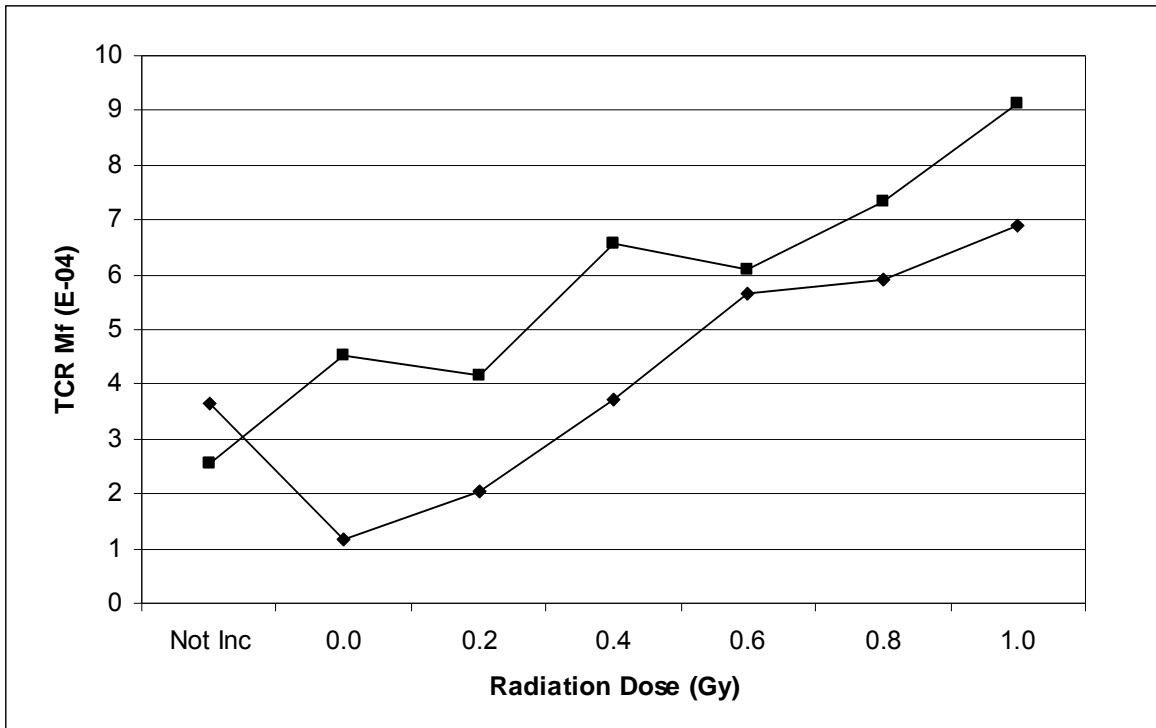


Fig. 7 Calibration of the TCR assay after incubation by *in vitro* irradiation.

The dose rate of irradiation was 0,589 Gy/min. “Not Inc” - stands for the Mf before incubation. Irradiation conditions – as described in “Methods”.

In addition the calibration test of irradiating the lymphocytes with doses ranging from 0 to 1 Gy was done (Fig. 7). Using these curves the individual dosimetry can be done but only if 1) there is linear dependency *in vivo* between Mf and dose up to the 1 Gy 2) if acute *in vitro* irradiation with ^{137}Cs source corresponds to the irradiation received by RIT.

3.3.1.2. Latent TCR mutants in patients treated with radioiodine

Based on the results of previous experiments, cells were incubated for 6 days. During this time they underwent around 5 divisions and the number of measured mutants was found to be at its maximum (see Fig. 6). After *in vitro* irradiation with 1 Gy the number of mutants quadrupled in comparison to non-irradiated sample. Also, the incubation itself had an influence on the base level of

mutants. As a rule the Mf after incubation in non-irradiated lymphocytes was lower than before (see Tab. 8). Also, occasionally the opposite effect was observed.

For measuring the radiation-induced TCR mutants after RIT 4 different lymphocyte probes were measured:

1. Lymphocytes from blood taken before RIT (Mf0)
2. Lymphocytes from blood taken before RIT and incubated for 6 days (Mf0•Inc)
3. Lymphocytes from blood taken before RIT, irradiated with 1 Gy and incubated for 6 days (Mf•1Gy•Inc)
4. Lymphocytes from blood taken 4 days after the begin of RIT and incubated for 6 days (Mf96•Inc).

Tab. 8 TCR-Mf of lymphocytes after *in vitro* incubation.

Probes	TCR-Mf x 10 ⁻⁴ (mean ± 1σ)	
	1. RIT (n=8)	2. RIT (n=13)
Dose (mSv)	176 ± 32	439 ± 106
Mf0	2.24 ± 0.71	3.77 ± 1.58
Mf0•Inc	1.54 ± 0.58	2.92 ± 1.44
Mf0•1Gy•Inc	9.10 ± 2.56	9.10 ± 3.12
Mf96•Inc	3.26 ± 0.76	6.51 ± 4.50

The analysis of all parameters was done by Sigma-Stat software. Patients treated for the 1st time were analysed separately, because the resulting Mf wasn't influenced by previous RITs. Two types of tests were used: Paired T-test and Wilcoxon Signed Rank Test. The paired T-test examines the changes that occur before and after a single experimental intervention on the same individual to determine whether or not the treatment had a significant effect. Examining the changes rather than the values observed before and after the intervention removes the differences due to individual responses, producing a more sensitive and powerful test. If the distribution of the observed effects was non-parametric, the Wilcoxon Test was used. A signed rank test ranks all the observed treatment

differences from smallest to largest without regard to sign (based on the absolute value), then attaches the sign of each difference to the ranks. The sign ranks are summed and compared. This procedure uses the magnitude of the effects and the sign. Paired t-test was preferred when possible (Tab. 9). As a rule, the following dependence for TCR-Mf was found: Mf0•Inc < Mf0 < Mf96•Inc << Mf0•1Gy•Inc.

Tab. 9 Comparison of TCR-Mf values after *in vitro* incubation

Probes	P-Value				Significance
	1. RIT		2. RIT		
	t-Test (paired)	Wilcoxon	t-Test (paired)	Wilcoxon	
Mf0•Inc vs Mf0•1Gy•Inc	<0.0001	< 0.0002	Impossible	<0,0001	+
Mf0•Inc vs Mf96•Inc	0.001	0.0003	0.016	0.0014	+
Mf0 vs Mf96•Inc	0.007	0.029	0.045	0.026	(+)
Mf0•Inc vs Mf0	0.11	0.054	0.16	0.13	-

3.3.2. Discussion (latent TCR mutants)

3.3.2.1. Shortening of the latent period

One of the inconveniences of TCR assay is that it could be used as a biological dosimeter only after a latent period of about half year after irradiation. This time is needed for mutated lymphocytes to express the mutant phenotype resulting in the absence of TCR on their surface. By *in vitro* incubation of the irradiated T-cells we can shorten this latent period to approximately one week.

Mutated lymphocytes are proliferating only if there is still CD3 receptor present on their surface. After a few divisions the cells with mutated receptor gene stop expressing CD3 receptor (at this moment they could be already detected by flow cytometry) and do not divide anymore, whereas normal cells continue to

proliferate. If cells are cultured for a longer time, the mutant cells are outnumbered by normal proliferating lymphocytes.

The goal of our experiments was to prove the possibility of TCR mutants detection in the lymphocytes of RIT patients shortly after exposure. Also, we optimized the protocol for *in vitro* culture of irradiated lymphocytes (Fig. 6) and established calibration curves for lymphocytes irradiated *in vitro* (Fig. 7).

3.3.2.2. Latent TCR mutants as a biodosimeter for recent exposure

For TCR assay after *in vitro* culture and irradiation the doubling dose (dose which doubles the rate of spontaneous mutations) can be found using the value from Tab. 8 in the Eq. 7. The calculated value is supported by earlier measurements of TCR-Mf in patients with latent period of at least 6 months after RIT.

$$\begin{aligned} \text{Doubling Dose (RIT)} &= \frac{RIT - Dose \times Mf0}{[Mf96 \bullet Inc - Mf0 \bullet Inc]} \\ &= \frac{176 \text{ mSv} \times 2.24}{3.26 - 1.54} = 229 \text{ mSv} \end{aligned} \quad \text{Eq. 7}$$

$$RIT - Dose = \frac{1000 \text{ mGy} \times [Mf96 \bullet Inc - Mf0 \bullet Inc]}{[Mf0 \bullet 1Gy \bullet Inc) - Mf0 \bullet Inc]} \quad \text{Eq. 8}$$

The dosimetry for 7 out of 8 patients with 1st RIT, according to Eq. 8, showed the result of 248 ± 50 mGy. This value is around 1.4 times higher than the value obtained by activity measurements (chapter 2.3.2.). In one patient dosimetry wasn't possible, because Mf0 Inc and Mf96 Inc were equal.

The *in vitro* incubation for early measurements of TCR-Mf is only possible in patients with no previous exposure to radiation. Described calculations were not possible in patients after the 2nd RIT. The values were either too high or too low to be in reasonable range. The reason being that the first RIT, which happened less

than half a year before the 2nd therapy, during the incubation gave rise to the extra mutants.

3.4. MN-Tf-Ret Assay

3.4.1. Results (MN-Tf-Ret Assay)

3.4.1.1. Flow cytometric measurements of micronucleated Tf-Ret

In the present investigation the frequency of micronucleated Tf-Ret was measured in patients during the RIT for thyroid cancer. All patients were children or young adults, who developed thyroid cancer years after the Chernobyl accident . Since Tf-Ret are very rare, they were immunomagnetically isolated from total blood before the determination of the f(MN-Tf-Ret) by flow cytometry. Fig. 8 shows the dot plots of Tf-Ret fractions before and after ^{131}I administration. Tf-Ret were isolated from about 1 ml blood. The purity of the Tf-Ret fraction is remarkable. The contamination by mature erythrocytes was below 10% in all preparations. The treatment induced a transitory increase in the frequency of MN-Tf-Ret.

3.4.1.2. Short time memory of MN-Tf-Ret Assay

Fig. 9 shows the f(MN-Tf-Ret) in patients before the 1st RIT or more than six months after the last treatment respectively. In 41 patients pre-treated for RIT 53 blood samples were taken at about 7 o'clock in the morning. Before RIT the mean f(MN-Tf-Ret) was $1.33 \times 10^{-3} \pm 1.01 \times 10^{-3}$ (mean \pm SD). Three outliers were found. Their frequencies were 4.2×10^{-3} , 4.4×10^{-3} and 5.5×10^{-3} , respectively. The f(MN-Tf-Ret) of patients who have already passed some RITs was not higher than in patients who have never been treated before. This indicates that the organism has a short memory for this radiation-induced mutation. There was no significant difference in f(MN-Tf-Ret) between males and females.

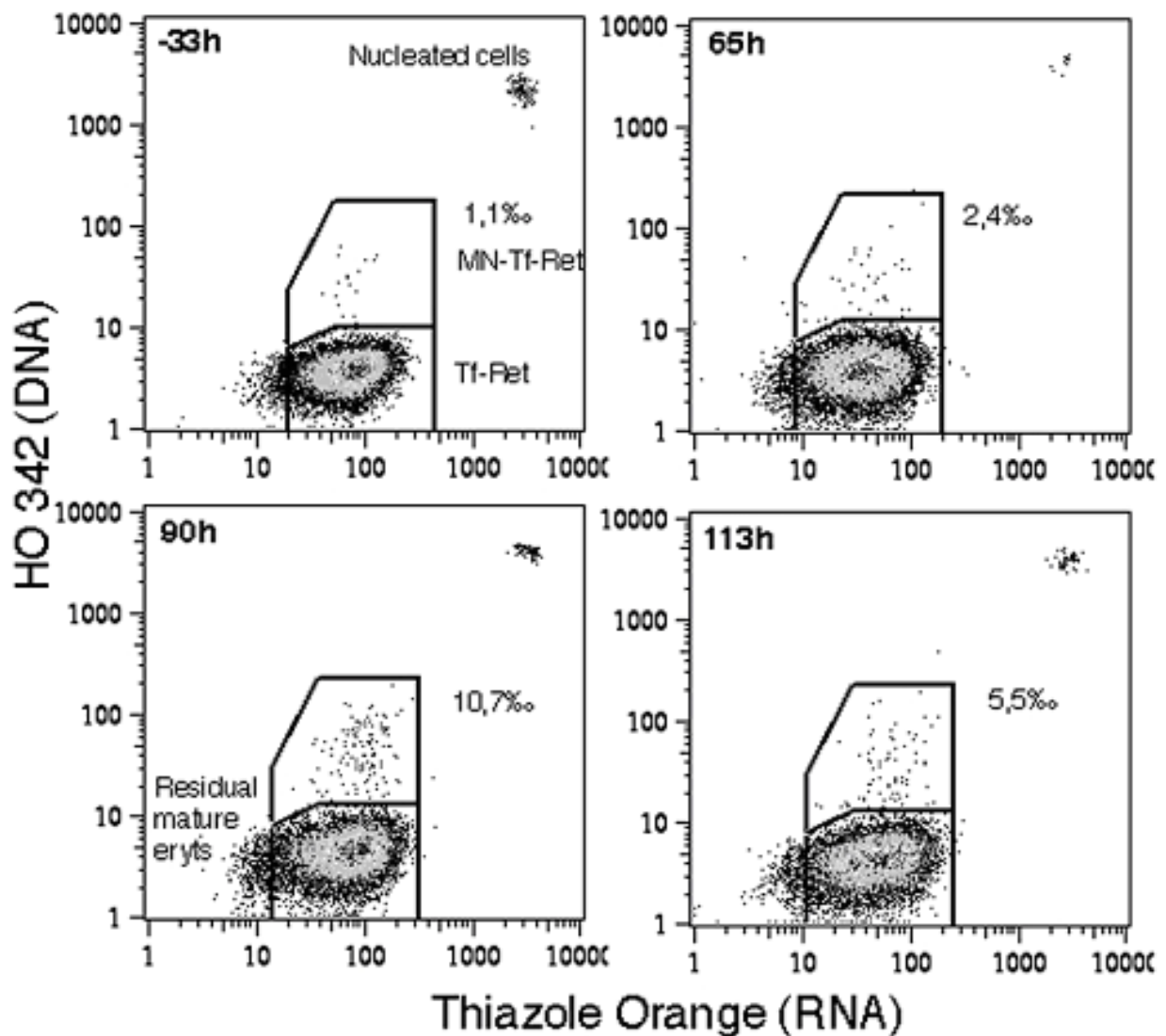


Fig. 8 Flow cytometric measurements of f(MN-Tf-Ret).

Flow cytometric dot plots of four Tf-Ret samples prepared from a representative patient (W010 – Tab. 5) before and after RIT. Hour indications (time points?) in each panel correspond to the time of ^{131}I administration. Tf-Ret isolation and flow cytometry are described in Methods. Each dot represents one cell. Values for the f(MN-Tf-Ret) are given for each time point. Axis X: Thiazole orange fluorescence (RNA); Axis Y: HO342 fluorescence (DNA).

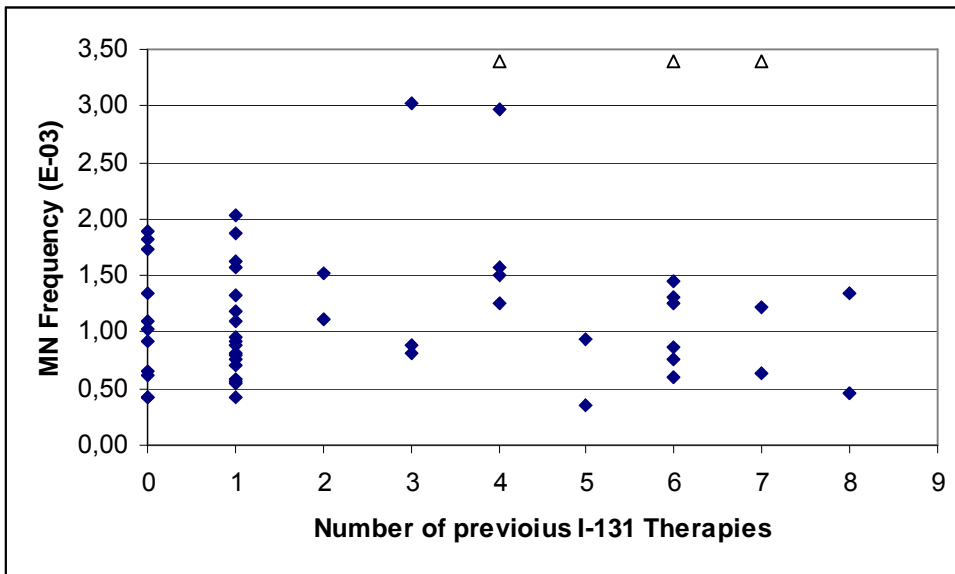


Fig. 9 f(MN-Tf-Ret) in patients before and 6 months after RIT.

f(MN-Tf-Ret) in patients treated for thyroid cancer before their 1st RIT or more than 6 months after their last one (N=53). In general, previous RITs didn't significantly increase the basal level of MN-Tf-Ret in blood. Three exceptions from this rule were found with f(MN-Tf-Ret) $4,18 \cdot 10^{-3}$, $4,44 \cdot 10^{-3}$ and $5,49 \cdot 10^{-3}$; they are labelled as white triangles.

3.4.1.3. MN-Tf-Ret mutant frequency during RIT

Typical time curves of f(MN-Tf-Ret) are presented in Fig. 10. Therapeutic ^{131}I activity about 50 MBq in the 1st RIT and about 100 MBq per kg BW in the following RITs were administered. The frequency was determined once a day. After a latent period of about 2 to 3 days MN frequency rose within one day to a maximum. Thereafter, it slowly decreased and reached the level before RIT within 3 to 6 days. The 'short transit' curves belong to two patients with an unusually short latent period.

Time curves of the f(MN-Tf-Ret) in patients who were prepared for RIT but only received a low diagnostic dose of ^{131}I as they did not need to be treated, showed no significant increase in MN-Tf-Ret. The dose to red marrow after ^{131}I diagnosis is about 20 mSv. This means that neither the radiation dose due to a

diagnostic ^{131}I application nor the small dose of the CT scan carried out before RIT to detect lung metastases significantly increases the $f(\text{MN-Tf-Ret})$.

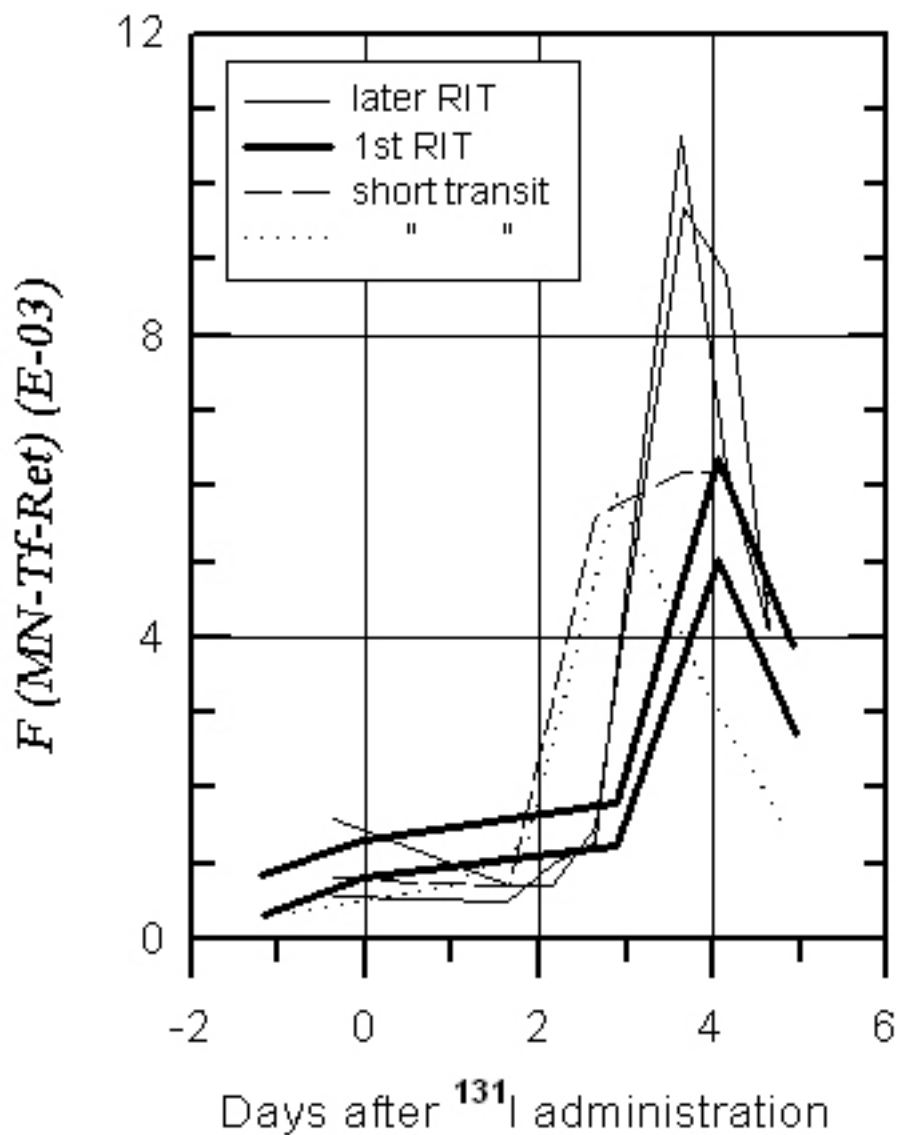


Fig. 10 Course of $f(\text{MN-Tf-Ret})$ after therapeutic ^{131}I application. Dotted curve (1st RIT) and dashed curve (2nd RIT) are from patients, where an increase of $f(\text{MN-Tf-Ret})$ was detected earlier than usual.

Tf-Ret are the youngest reticulocyte cohort in blood. Under steady state conditions the number of Tf-Ret that enters blood per minute is equal to the number of mature reticulocytes that are transformed to erythrocytes. It was investigated, if RIT can impair this equilibrium. During the 1st RIT the frequency of reticulocytes remained constant, as should be expected, if RIT does not disturb erythropoiesis.

3.4.1.4. Red marrow radiation dose and f(MN-Tf-Ret)

Tab. 10 gives the values of the f(MN-Tf-Ret) as well as of the radiation dose to RM in 5 male patients for their first and second RIT, which were performed 9 months apart. The RM-dose in the second RIT was more than 2 times higher than in the first one. The maximal measured f(MN-Tf-Ret) after the second therapy was almost twice as that after the first RIT. However, due to the large inter-individual variability as well as low number of patients, whose data were available from more than one RIT, the difference in response between the two treatments was of low significance ($p=0.03$, one-sided sign test).

The relationship between the dose rate of red marrow irradiation and the f(MN-Tf-Ret) in peripheral blood for two male patients with normal (left) and delayed iodide excretion (right) is shown in Fig. 11 The corresponding residence time of ^{131}I in the body (τ_{TB}) was 16.9 h and 38.0 h respectively. In the patient with delayed excretion the total dose to RM was much higher than in one with normal excretion, though the activity given per kg BW was lower.

The upper part of the figure shows that MN-Tf-Ret entered blood, when the dose rate of irradiation was already quite low. The figures in the middle give the relationship between the total dose to RM and the dose during the last 24 h. Such interval was chosen because the cell cycle of an erythroblast lasts about 24 h [32, 33]. The height of maxima of the 24 h dose curves are quite similar in both patients though the value of the total RM dose in one patient was two times higher than in the other. The shapes of the 24 h dose curves resemble the time curve of f(MN-Tf-Ret) in RIT (Top).

Tab. 10 f(MN-Tf-Ret) in five about 19 year old male patients during their 1st and 2nd RIT

Patient	1st RIT					2nd RIT								
	Dose mSv	f(MN-Tf-Ret) (o/oo) hours after ¹³¹ I				Dose mSv	f(MN-Tf-Ret) (o/oo) hours after ¹³¹ I administration							
		0	70	96	118		- 7	41	53	65	89	101	113	
W229	185	1.3	1.8	6.4	3.9	356	0.6	0.5	0.6	1.4	2.3	10.7	2.1	
W230	199	2.9	2.1	11.5	4.5	479	1.0	1.0	1.5	3.3	13.2	8.2	9.1	
W231	207	0.8	1.2	5.0	2.7	473	1.9	0.6	0.7	2.0	9.2	20.5	4.9	
W232	168	0.9	2.1	7.2	3.3	329	2.0	1.2	1.6	4.2	18.6	16.8	4.4	
W233	183	0.8	1.0	9.6	4.3	350	1.6	0.7	0.7	1.5	9.7	8.8	4.1	
Mean	188	1.3	1.6	7.9	3.7	397	1.4	0.8	1.0	2.5	10.6	13.0	4.9	
SD	15	0.9	0.5	2.6	0.7	73	0.6	0.3	0.5	1.2	6.0	5.4	2.6	

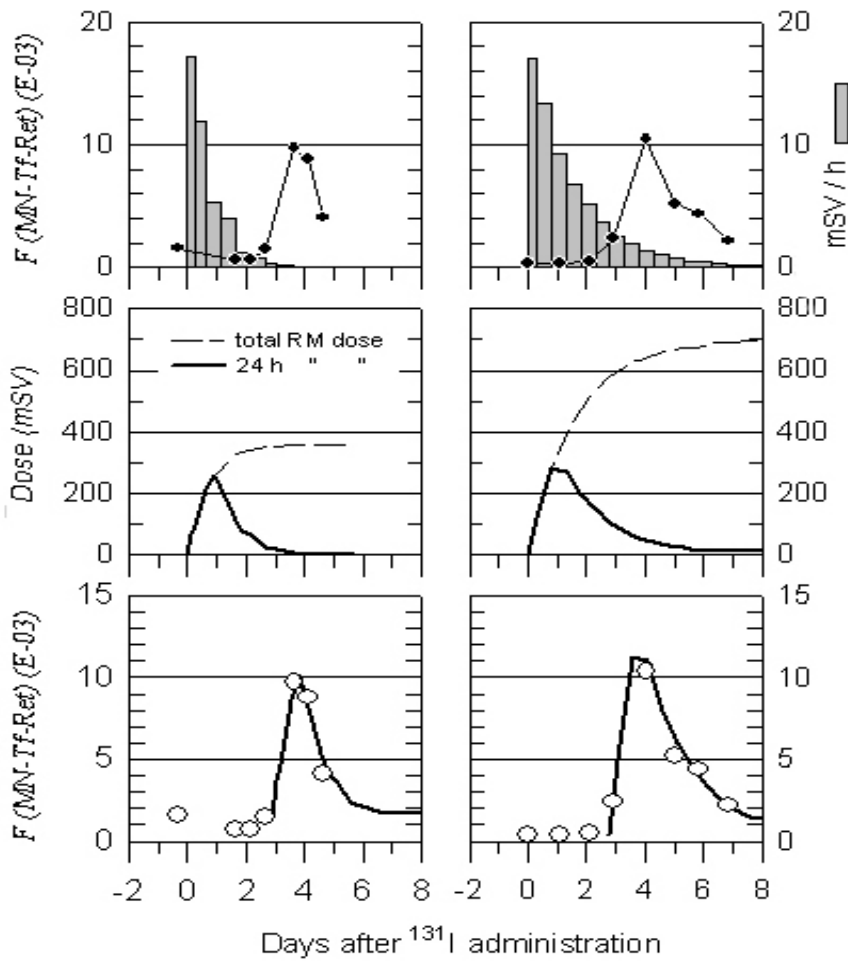


Fig. 11 Relationship between the radiation doses to red marrow and $f(\text{MN-Tf-Ret})$ in the blood of a patient with normal (left) and slow (right) radioiodine excretion. The ^{131}I activity applied was 101 MBq (left) and 82 MBq (right) per kg BW, respectively.

Top : $f(\text{MN-Tf-Ret})$ in blood and dose rate to RM.

Middle : Cumulative radiation dose to RM and RM dose within the last 24 h of RIT.

Bottom : Measured and simulated time curve of $f(\text{MN-Tf-Ret})$.

In simulations the probability for the induction of a micronucleus (P_{MN}^*) were 3.3×10^{-5} (left) and $3.9 \times 10^{-5} \text{ mSv}^{-1}$ (right) respectively. The latent interval L was 63 h (left) and 67 h (right) respectively. Details of the simulation are given in Section 3.4.2.4.

Simulated MN-Tf-Ret time curves are given at the bottom. Simulated curves fit quite well to the measured $f(\text{MN-Tf-Ret})$. Similar fits were done in 17 male and 12 female patients respectively.

Fig. 12 shows the dose dependence of $f(\text{MN-Tf-Ret})$. The values between 110 and 220 mSv are related to the first RIT whereas all others belong to second or later therapies. Within the dose range of 100 to 600 mSv the dose dependence is poor. The bold line is the linear regression line for all data. Its parameters as well as those of the gender specific regression lines are given in Tab. 11. On average, the dose dependent increase of MN frequency in men is higher than in women.

Tab. 11 Dose dependence of $f(\text{MN-Tf-Ret})$ in patients after RIT in Fig 12.

Parameters of the regression line $f(\text{MN} \cdot \text{Tf Ret}) = Y_0 + a \times D$

Gender	RITs n	Y_0 $\times 10^{-3}$	SE*	a (mSv ⁻¹) $\times 10^{-5}$	SE*	R ²	Doubling Dose (mSv)
Man	24	1.58	0.53	2.27	0.22	0.69	70
Women	26	1.39	0.53	1.52	0.21	0.52	91
both	50	1.55	0.40	1.86	0.16	0.58	83

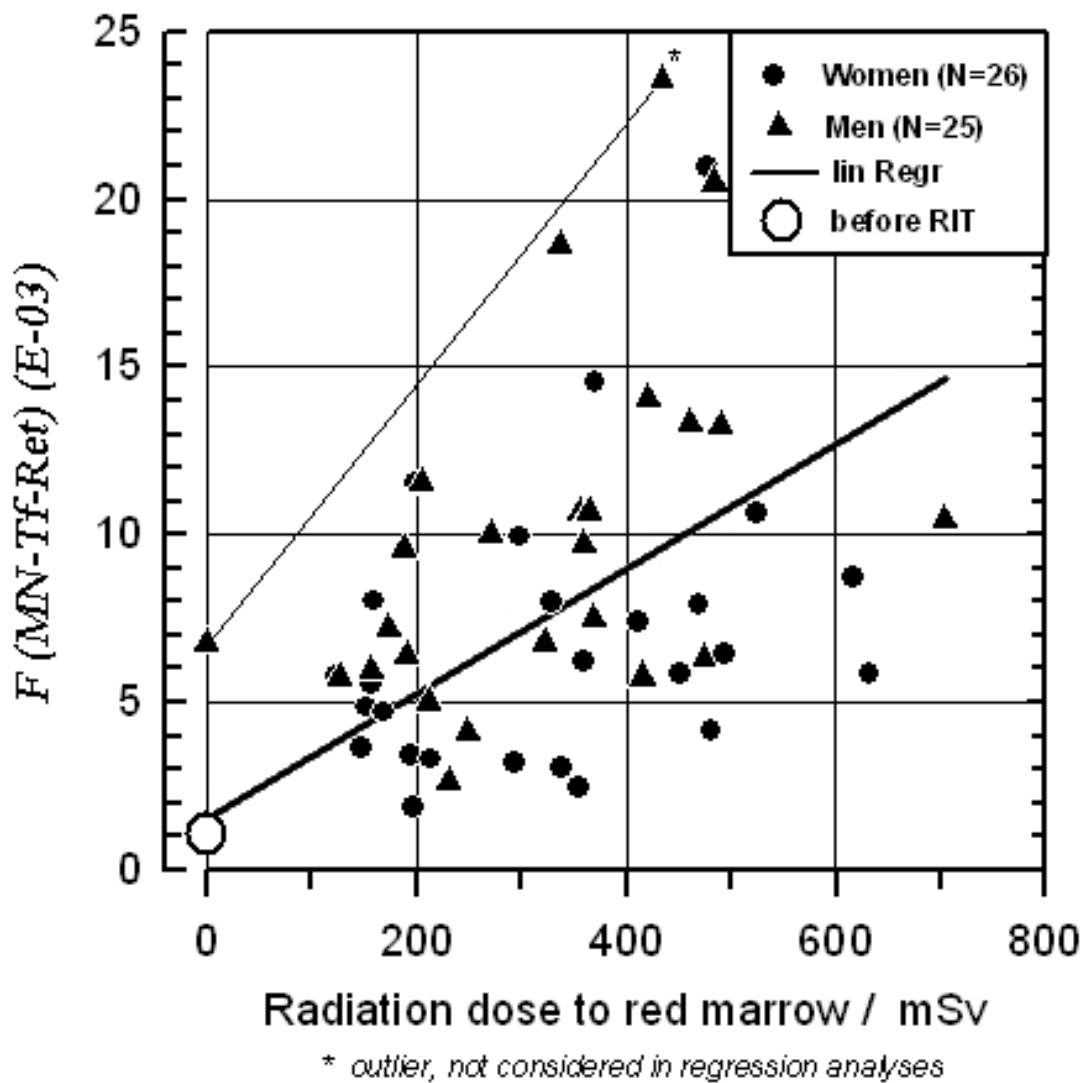


Fig. 12 Dose and gender dependence of $f(\text{MN-Tf-Ret})$ in RIT.

For 51 RIT in 24 women and 22 men the MN frequency in the maximum 3 to 4 days after ^{131}I administration and the corresponding frequency before treatment are given as a function of the total RM dose (Tab. 11). The bold line is the linear regression line for the data of all RITs except one.

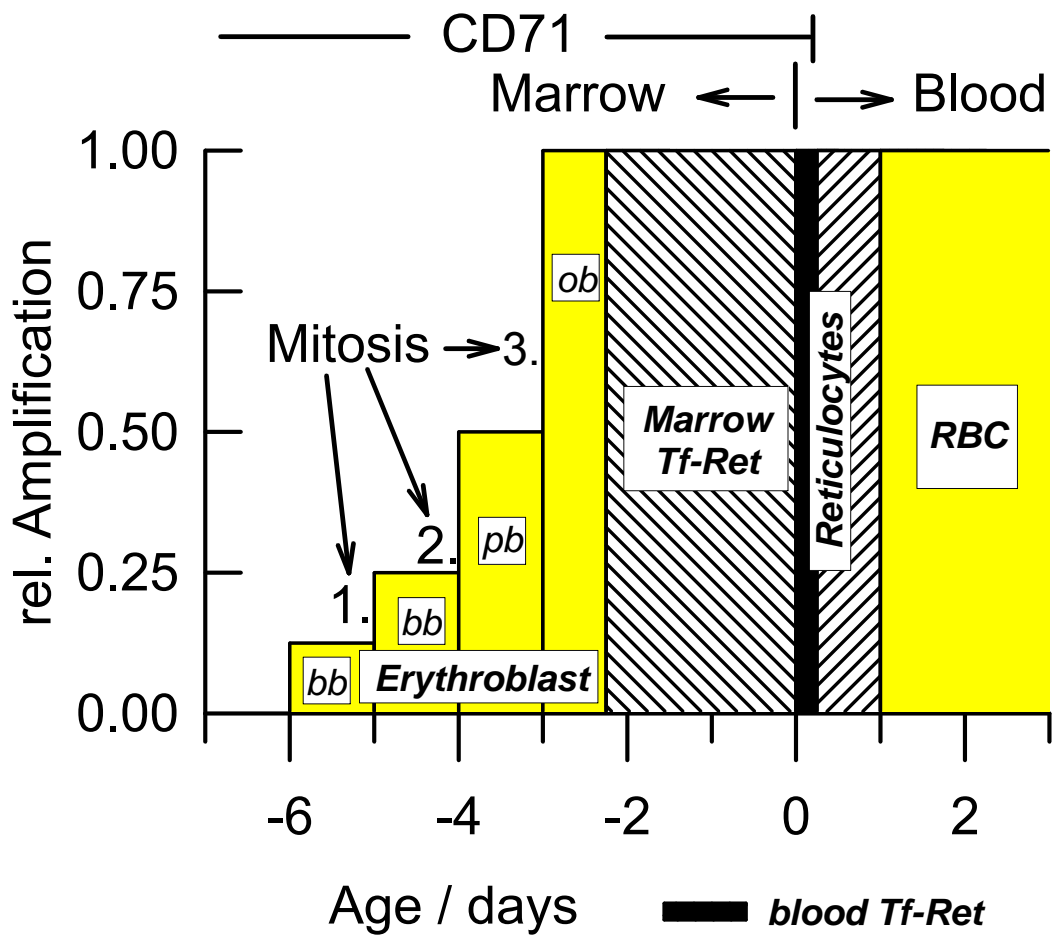


Fig. 13 Timetable of erythropoiesis in man and relative frequency of red blood cell (RBC) precursors according to investigations with radiothymidine and radioiron [32, 33].

The day, when reticulocytes enter the blood was taken as zero. Most micronuclei arise at the last mitosis. They arrive in blood about 70 h later.

Bb - Basophilic E. pb - Polychromatic E. ob - Orthochromatic Erythroblast

3.4.2. Discussion (MN-Tf-Ret assay)

3.4.2.1. Transferrin positive reticulocytes in blood as a part of erythron

The knowledge of the timetable of erythropoiesis is a prerequisite for the understanding of the course of $f(\text{MN-Tf-Ret})$ in radioiodine treated patients. An overview of the size of the different cell fractions of the erythron and the timetable of the erythropoiesis is given in Fig. 13. Term erythron refers to the combined populations of erythrocytes and their haemoglobin containing precursors in blood and bone marrow. The scheme is based on investigations with radiothymidine and radioiron, which selectively label all haemoglobin producing and proliferating cells [32, 33]. Tf-Ret in blood is a very small fraction of the erythron. They resemble Tf-Ret in marrow in cell size and by the presence of cytoplasmic organelles (mitochondria and ribosomes) and of transferrin receptors. In blood they belong to the so-called immature reticulocyte fraction [34].

3.4.2.2. Role of lifespan of Tf-Ret in peripheral blood

In the present investigation $f(\text{MN-Tf-Ret})$ in blood was measured as an indicator of the $f(\text{MN-Tf-Ret})$ in marrow, where radiation induced MN arise at the mitosis of an erythroblast. The red pulp of the spleen plays a key position in the maturation of Tf-Ret and elimination of MN-Tf-Ret, since it temporally sequesters reticulocytes [35] and removes micronucleated ones. In erythrocytes of patients, whose spleen has been removed, not only micronuclei (Howell-Jolly bodies) but also autophagosomes containing mitochondria and ribosomes were found [36]. Autosomes are normally absent from mature erythrocytes.

The relationship between the $f(\text{MN-Tf-Ret})$ in blood and marrow is described by Eq. 9a and Eq. 9b. It takes into account the fact that under steady state condition the number of erythrocytes of a cohort in blood is equal to the product of the respective entrance rate Δ ($\text{cells} \times \text{min}^{-1}$) and the corresponding average lifespan τ . In Eq. 9b τ values were substituted by the rate constant of transformation of Tf-Ret to mature reticulocytes (α_1) and the rate constant of disappearance MN-Tf-Ret in the spleen

(α_2), where $\tau_{Tf-Ret}=1/\alpha_1$ and $\tau_{MN-Tf-Ret}=1/(\alpha_1+\alpha_2)$. The ratio of the entrance rates from red marrow to blood in Eq. 9a and 9b is approximately equal to the $f(MN-Tf-Ret)$ in red marrow. The value $f(MN-Tf-Ret)$ in blood can only be taken as an indicator of $f(MN-Tf-Ret)$ in red marrow, if $\tau_{Tf-Ret} \approx \tau_{MN-Tf-Ret}$ or $\alpha_1 \gg \alpha_2$. That this condition might be fulfilled is supported by comparing the present data on

$$\left[\frac{MN \cdot Tf \ Ret}{Tf \ Ret} \right]_{Blood} = \left[\frac{\Delta(MN \cdot Tf \ Ret)}{\Delta(Tf \ Ret)} \right]_{RM} \times \frac{\tau_{MN \cdot Tf \ Ret}}{\tau_{Tf \ Ret}} \quad \text{Eq. 9a}$$

$$= \left[\frac{\Delta(MN \cdot Tf \ Ret)}{\Delta(Tf \cdot Ret)} \right]_{RM} \times \frac{\alpha_1}{\alpha_1 + \alpha_2} \quad \text{Eq. 9b}$$

baseline $f(MN-Tf-Ret)$ with data on micronucleated polychromatic erythrocytes (MN-PCE) in bone marrow smears from control persons [37]. The MN-Tf-Ret values are only slightly lower than the MN-PCE values, and this small difference may be due to the different scoring methods (flow cytometric vs. microscopic) and/or to the lower age of the persons sampled in the present study.

3.4.2.3. Radiation dose per cycle and $f(MN-Tf-Ret)$ in blood

After ^{131}I administration three typical phases can be discriminated in the course of $f(MN-Tf-Ret)$ (Fig. 14A). During the first phase, the latent period L, $f(MN-Tf-Ret)$ stays at the basal level. It lasts approximately 3 days. The length of the latent period corresponds to the transition time required by an orthochromatic erythroblast for nucleus extrusion and reticulocyte maturation in marrow (Fig. 13). The next phase is characterised by a rapid rise in MN frequency from the basal level to the maximum. Its duration is about one day. Within the last phase $f(MN-Tf-Ret)$ slowly declines to the basal level within several days. The length of this phase is the most variable.

This time course of $f(MN-Tf-Ret)$ can be understood if i) MN arise only in the last erythroblast mitosis and ii) if $f(MN-Tf-Ret)$ in blood is proportional to the radiation dose during the last erythroblast cell cycle, which lasts approximately

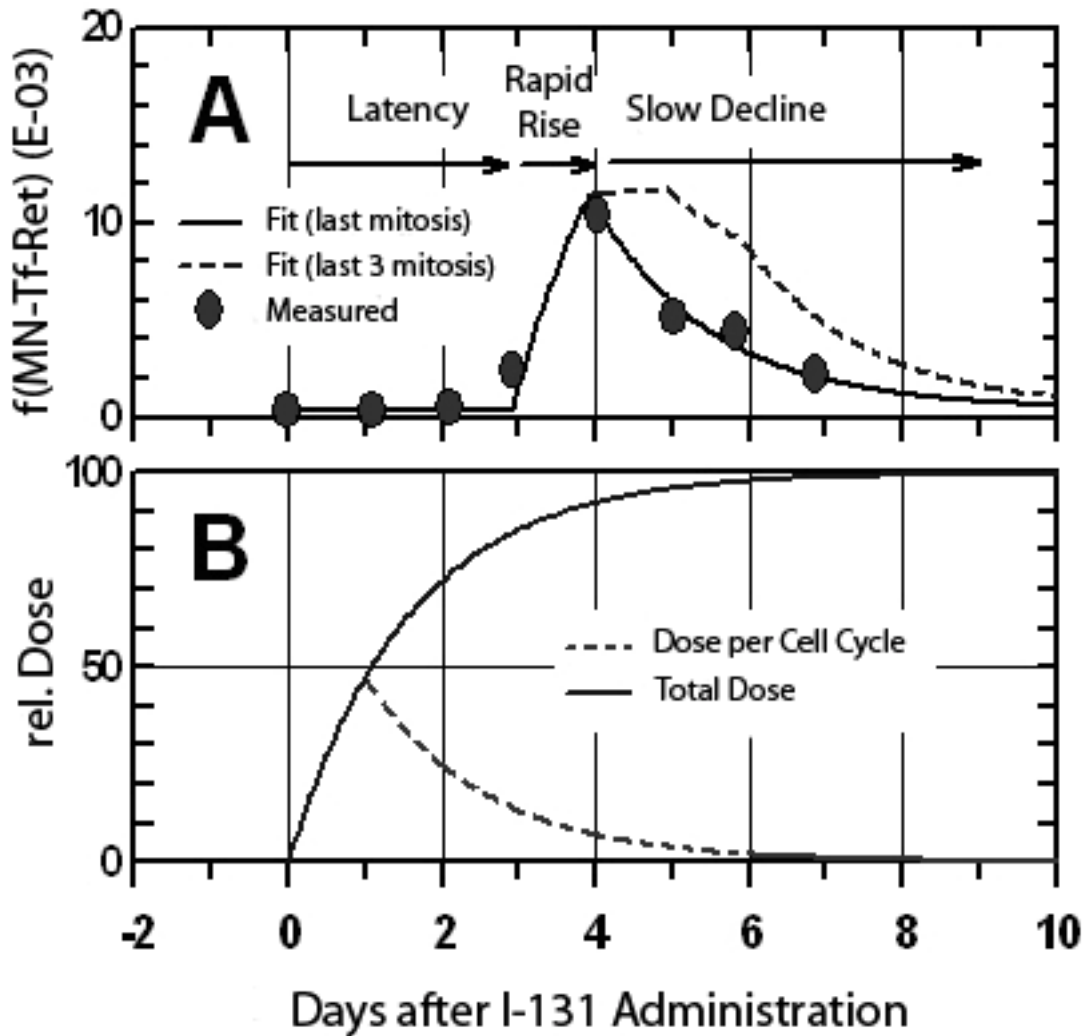


Fig.14 The course of radiation induced MN-Tf-Ret in blood after radioiodine administration.

A. $f(\text{MN-Tf-Ret})$: The course is characterised by a latent period of approx 3 days, a rapid rise in frequency between day three and four and a slow decline in the following days. Curves were fitted to the data of a patient under the assumption of a latent period of 70 h, an erythroblast cell cycle time of 24 h. The value of P_{MN} was $4.6 \times 10^{-5} \text{ mSv}^{-1}$.

B. Radiation dose: Time dependence of the radiation dose per cell cycle (cycle time 24 h) and the total dose to red marrow.

24 hours (Fig. 14b). Immediately after the latent period the first radiation induced MN-Tf-Ret enter the peripheral blood. In the beginning their frequency is low, since the corresponding erythroblasts were irradiated only for a short part of their cell cycle. In the following rapid rise of $f(\text{MN-Tf-Ret})$, Tf-Ret that descend from erythroblasts exposed for a longer period of the cell cycle enter blood. In the maximum of MN-frequency Tf-Ret are for the first time descendants of erythroblasts, which were exposed during the whole cycle. They have the highest dose per cell cycle of all (Fig. 14b). Later on the dose per cell cycle decreases. This explains the slow decline in $f(\text{MN-Tf-Ret})$.

Occasionally, we found patients after RIT who had a shorter latent period. Two examples are given in Fig. 10. In both patients the haematological markers (haemoglobin, hematocrit) argue in favour of an iron deficient erythropoiesis and anaemia respectively [34]. Anaemia shortens the transit time of reticulocytes [32]. Recently some data on the time course of $f(\text{MN-Tf-Ret})$ during a radiotherapy or chemotherapy in cancer patients have been published [38]. In most of these patients the length of the latent period was shorter than in the present investigation, because patients were exposed to acute radiation and most likely were anaemic.

3.4.2.4. Model describing the time- and dose-dependence of $f(\text{MN-Tf-Ret})$

The model is based on the following assumptions, most of which are fulfilled in mice for clastogenic agents [39, 40]:

1. MN are induced by radiation during all phases of the cell cycle.
2. MN becomes apparent in the first post-injury mitosis and can be seen in the following interphases.
3. The erythropoietic system is in a steady-state and radiation dose not disturbed it;
4. Radiosensitivity for MN-induction does not vary throughout the cycle.
5. $f(\text{MN-Tf-Ret})$ increases linearly with the radiation dose.

Under these assumptions, the dose- and time-dependency of $f(\text{MN-Tf-Ret})$ in blood t hours after radioiodine administration ($f(\text{MN-Tf-Ret})_{D,t}$) is given by Eq. 10.

$$f(\text{MN} \cdot \text{Tf} \cdot \text{Ret})_{D,t} = f(\text{MN} \cdot \text{Tf} \cdot \text{Ret})_{\text{spont}} + \\ + P_{MN}^* \times (D_{CT,t-L} + 0.5 \times D_{CT,t-L-T} + 0.25 \times D_{CT-L-2T}) \quad \text{Eq. 10}$$

$$P_{MN}^* = P_{MN} \times \frac{\tau_{\text{MN} \cdot \text{Tf} \cdot \text{Ret}}}{\tau_{\text{Tf} \cdot \text{Ret}}} \quad \text{Eq. 11}$$

$$P_{MN}^* = \frac{f(\text{MN} \cdot \text{Tf} \cdot \text{Ret})_{\text{max}} - f(\text{MN} \cdot \text{Tf} \cdot \text{Ret})_{\text{spont}}}{D_{CT\text{max}}} \quad \text{Eq. 12a}$$

$$P_{MN}^* \approx \frac{(10.4 - 0.4)}{330} = 3.03 \times 10^{-5} \quad \text{Eq. 12b}$$

P_{MN} is the probability that an erythroblast, which arises at mitosis, contains a micronucleus, if the progenitor cell was exposed to a dose of 1 mSv during its last cell cycle. The relationship between P_{MN}^* and P_{MN} is given by Eq. 11. P_{MN}^* is equal to P_{MN} , if the lifespan of MN-Tf-Ret ($\tau_{\text{MN} \cdot \text{Tf} \cdot \text{Ret}}$) and $\text{Tf} \cdot \text{Ret}$ ($\tau_{\text{Tf} \cdot \text{Ret}}$) in blood are the same. $D_{CT,t}$ is the dose per cell cycle t hours after RIT begin, L the duration of the latent period and T the cell cycle time. The parameters in brackets give the contribution of micronuclei arising after the third, second or first erythroblast mitosis (Fig. 13), if the cell cycle time in all erythroblast generation is 24 h and if no cells are lost by apoptosis. The value of the highest measured $f(\text{MN-Tf-Ret})$ permits a first guess of the value of P_{MN}^* (Eq. 12a). For the patient whose data are given in Fig. 14a the approximate value of P_{MN}^* is $3.0 \times 10^{-5} \text{ mSv}^{-1}$ (Eq. 12b), if the cell cycle lasts 24 h. When values for P_{MN}^* , L and the time curve of D_{CT} are known, the course of $f(\text{MN-Tf-Ret})$ can be calculated.

The bold curve in Fig. 14a shows the time dependence of $f(MN \cdot Tf \ Ret)_{D,t}$ for this patient, if micronuclei are only induced during the cell cycle before the very last erythroblast mitosis. The calculated curve fits to the measured values rather well. The dashed curve shows the result of a simulation where it was assumed that MN from the last three erythroblast divisions enter the blood. Under this assumption the peak of $f(MN-Tf-Ret)$ is significantly broader than actually measured. Similar results were found in all patients, where a sufficient number of measurements of $f(MN-Tf-Ret)$ were available to define the time-curve. Therefore, we assume that most MN found in Tf-Ret arise at the very last erythroblast division. Erythroblasts, in which a MN arises in an earlier mitosis, might die. This ineffective erythropoiesis is quite normal in human bone marrow. About 10% of the maturing cells die in this way [41]. The calculation was performed for an erythroblast cycle time of 24 hours sharp. Our data don't allow to decide if CT is a little shorter or longer than 24 h, since in most patients $f(MN-Tf-Ret)$ was only measured once a day. For the same reason it is rather improbable that the time and height of the measured MN maximum will correspond to the data of the real MN peak. In general, the highest measured value will be significantly lower than the real maximum.

Tab. 12 gives the mean values of P_{MN}^* found in men and women after RIT. The values were calculated by Eq. 12a. There is a significant gender specific difference in P_{MN}^* ($P < 0.005$). According to Eq. 9a, differences in the lifespan of MN-Tf-Ret and Tf-Ret in blood as well as well gender specific differences in radiosensitivity might be the reason. In conclusion, higher doses are needed for women to reach the same MN frequency as men. This possibility, however, seems to be rather unlikely. Other publications on MN [42-44] support the point that the baseline MN frequencies in women are higher than those in men and there is no difference in radiosensitivity between genders. However, in this publication the MN were measured in lymphocytes and not in reticulocytes. It is possible that the RM doses in women were systematically overestimated.

Tab. 12 Value of P_{MN}^* in patients after RIT

Statistics	$P_{MN}^* \times 10^{-5}$ (mSv ⁻¹)	
	Men (N=25)	Women (N=25)
Mean \pm SD	3.8 \pm 1.5	2.5 \pm 1.4
Median	4.0	2.2
Range	1.3 - 6.6	0.7 - 6.3

3.4.2.5. Adaptation of the model to MN in polychromatic erythrocytes in mice

The counterparts to the reticulocytes in the human blood are the polychromatic erythrocytes (PCE) in mice. They represent immature erythrocytes with a lifespan in peripheral blood of about 15 h [45]. Contrary to MN-Tf-Ret in human, MN-PCE are not cleared by the mouse spleen [46]. As a consequence, the lifespan of MN-PCE and PCE in blood are the same. In this case P_{MN}^* and P_{MN} are equal. Many investigations on the MN-induction by ionizing radiation were done in mice [45, 47-53]. Fig. 15 gives examples for the MN-PCE frequency in blood of mice after acute [45] and chronic [54] radiation respectively. Each point in the left part of Fig. 15 represents one irradiated animal. The little scatter of the data indicates that in inbred animals the interindividual variation of radiosensitivity is small. The time curves were simulated using the kinetic data of mouse erythropoiesis and P_{MN} values, which were hardly higher than the P_{MN}^* in human. The calculated curves fit remarkably well to the published data. This supports the notion that at least in experiments with ionizing radiation the MN-PCE test in mice can be used as a model for the MN induction in human erythroblasts.

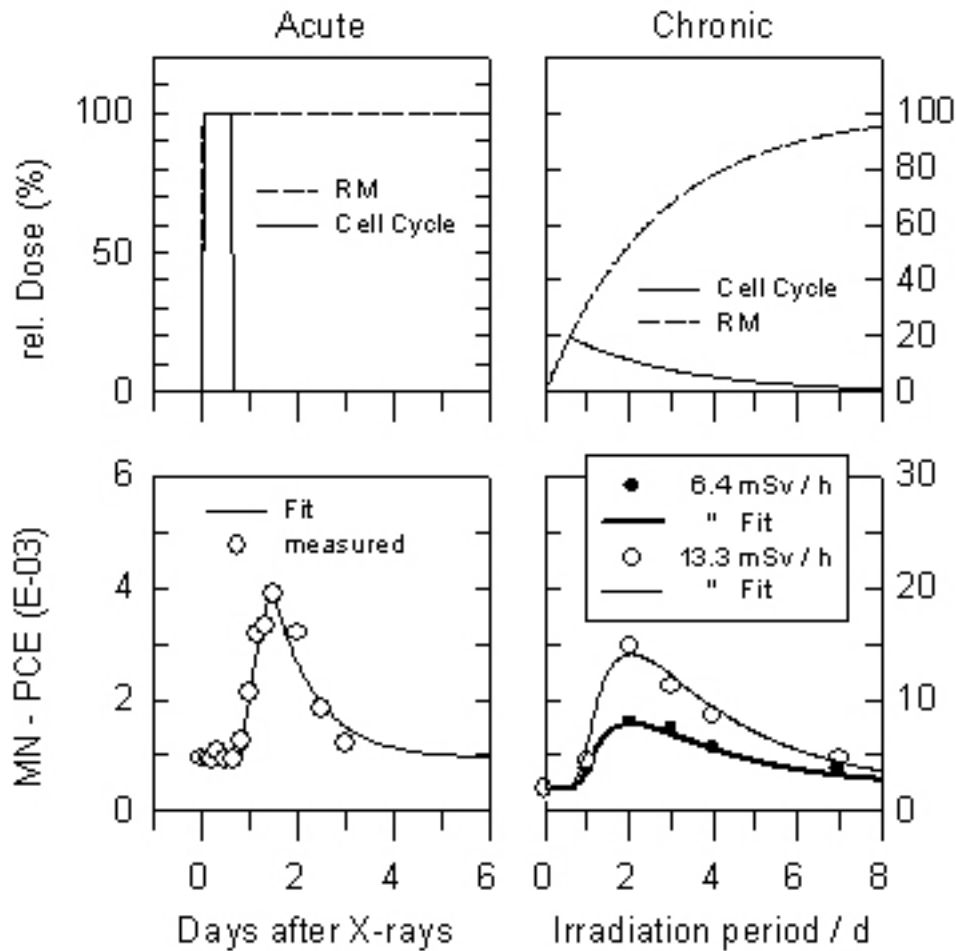


Fig. 15 Measured and simulated frequency of MN-PCE in peripheral blood of mice as a function of time after irradiation.

Left.: Acute irradiation with 100 mSv X-rays. MN-PCE were measured by FCM. Data were taken from [45].

Right: Chronic irradiation with an external ^{137}Cs γ -irradiator. Dose rate was decreased exponentially, with $T_{1/2}$ of 64 h. The maximum total dose per cell cycle was 116 and 241 mSv respectively. Data were taken from [54]. MN-PCE frequency as determined microscopically after staining with acridine orange.

The following cytokinetic data were used in acute and chronic irradiation, respectively: CT of the last erythroblast stage 15 and 14 h, reticulocyte maturation time in bone marrow 20 and 14 h, half life of PCE in blood 15 and 10 h. The value of P_{MN} was 6×10^{-5} and $7 \times 10^{-5} \text{ mSv}^{-1}$.

animals: acute: male CBA-S mice aged 7-8 weeks

chronic: female Swiss Webster mice aged 6-7 weeks

3.4.2.6. Features of the MN-Tf-Ret assay

As explained above, the increase in $f(\text{MN-Tf-Ret})$ in irradiated people should be an indicator of the radiation dose during a distinct time interval, namely the last erythroblast cell cycle. As a consequence, this assay is a biological dosimeter, which allows to measure the total radiation dose during a time interval that corresponds to the average cell cycle time of a polychromatic erythroblast (Fig. 13). Measurements in blood are not possible until the latent period of about 3 days has passed. This feature distinguishes the MN-Tf-Ret assay from most other common biological dosimeters such as cytogenetic assays [55], MN in lymphocytes [56, 57], or assays that measure somatic mutations in blood cells (GPA-, HLA-, HPRT-, or TCR assay) [9]. All these assays are cumulative biological dosimeters, which have the potency to determine the total dose accumulated within months to years. The MN-Tf-Ret test is not specific for ionizing radiation. In mice MN-PCE test was able to register the whole range of genotoxic effects from different chemical compounds [58, 59].

In the present investigation the dose dependence of $f(\text{MN-Tf-Ret})$ was weak. One reason is that in the present study only a narrow dose range was available for study - about 100 to 600 mSv. Also, the relationship between the dose-rate of radiation during RIT, and the sampling frequency influences the results. Dose-rate decreases exponentially corresponding to the effective half-life of ^{131}I in the patient. Under this condition $f(\text{MN-Tf-Ret})$ displays a dose dependent maximum, the height of which is proportional to the maximum dose per erythroblast cell cycle. As samples were normally taken only once a day, we should have missed the maximum in most patients. Shorter sampling intervals are, therefore, needed. Even if we knew the time of maximum response, there would be further uncertainty regarding the total dose to red marrow, which can be up to twice as high as the dose per cell cycle.

After acute irradiation it should be easier to find the precise dose dependence. In this situation the dose per cell cycle is constant and equal to the

total dose to red marrow. While the construction of a calibration curve based on *in vitro* exposure is at present not feasible, a study of patients receiving defined acute whole-body exposures in the region of 0.1 – 1 Gy would be expected to give a more usable dose-response calibration curve. Additionally, a constant, chronic or subchronic exposure would in principle give a plateau after an initial latent period followed by a period of increase.

There are some features that may make the MN-Tf-Ret assay most useful as a biological dosimeter in humans. One is the high sensitivity of the assay, which allows the detection of radiation doses as low as 100 mSv. Another advantage under some exposure circumstances is the short memory of this endpoint. After exposure $f(\text{MN-Tf-Ret})$ returns to normal within a fortnight. This allows the retrospective comparison between the spontaneous and the radiation induced $f(\text{MN-Tf-Ret})$ on an individual base. The assay also has a well-documented animal model counterpart. Finally, the assay can be performed within three days. Thus, the method may be of use for monitoring individuals after suspected accidental radiation exposure, providing blood samples can be obtained during a few days after the presumed exposure.

3.5. Biological dosimetry in radioiodine treated patients

Table 13 gives a short synopsis of biodosimetry in patients after RIT. Beside the assays used in the present investigation other methods were applied. They include:

1. MN in lymphocytes assay [60-67].

For this assay lymphocytes are cultured for 44 hours. Afterwards cytochalasin B is added. It blocks cytokinesis and makes possible the detection of lymphocytes dividing in culture. Cells that have undergone the first mitosis are recognised as binucleated, and they are screened for presence of micronuclei.

Tab. 13 Biological dosimetry in radioiodine treated patients

Assay	Doubling Dose mGy	Time interval of applicability	Biodosimeter characteristic	Time consume
MN-Tf-Ret * Assay	70 - 100	3 - 4 d	Recent	2 d
Standard * TCR assay	200 - 300	0,5 – 5 y	Cumulative	6 h
TCR assay * after cell culture	200 - 300	1 d – 3 mo ?	Cumulative	1 w
GPA assay *	500 - 600	0,5 y -∞	Cumulative	3 d
MN-Assay in Lymphocytes **	100	1 d –6 mo	Cumulative	3 d
Chromosome ** Aberrations	200	1 d –1 y	Cumulative	3 d

* Detection of altered cells by flow cytometry

** microscopic detection

2. Chromosome aberrations assays [68-75].

Fluorescence in Situ Hybridisation (FISH). Stained chromosome slides are analysed under the fluorescence microscope by visual scoring of translocations, insertions, deletions and breaks.

Sister chromatid exchange (SCE) method. The test is based on the exchange of 5-bromodeoxyuridine with thymine nucleotide in the chromosomes of newly multiplied lymphocytes. The chromosomal uptake site of the 5-bromodeoxyuridine does not permit staining, while thymine does.

3. Glycophorin A Assay [7, 51, 76, 77].

The glycophorin A (GPA) assay concurrently detects and quantifies two types of erythrocytes with variant phenotypes at the autosomal locus responsible for the polymorphic MN blood group. It uses a pair of allele-specific monoclonal

antibodies and flow cytometry to analyse a standard population of 5 million cells efficiently. The two phenotypes detected are simple allele loss and allele loss followed by reduplication of the remaining allele; both are consistent with the mechanisms underlying "loss of heterozygosity" at tumour suppressor genes.

The data in the table 13 demonstrate that TCR assay and the MN-Tf-Ret assays are potent methods for biological dosimetry. Their use could be recommended for monitoring of radiation therapy and radiation accidents.

4. Summary

In radiation accidents biological methods are used in dosimetry, if the radiation dose could not be measured by physical methods. The knowledge of individual dose is a prerequisite for planning a medical treatment and for health risk evaluations.

In the present work two biodosimetric assays were calibrated in young patients who were treated with radioiodine for thyroid cancer. Patients were from Belarus. They suffered from radiation induced thyroid cancer as a consequence of the Chernobyl reactor accident.

In radioiodine therapy (RIT) bone marrow and lymphatic organs are exposed to ionizing radiation at doses of 0.1 to 0.75 Sv within about 2 days. Since several RIT have to be applied with interval between each of them from 6 months up to approximately 1 year, total dose can be up to 2 Sv within 2 to 3 years. The dose for thyroid tissue is approximately 1000 times higher.

The dose-response relationship was measured by the T-cell receptor test (TCR test) in T4 lymphocytes with and without *in vitro* incubation or by the micronucleus assay in transferrin receptor positive reticulocytes (MN-Tf-Ret test). In all these assays, the frequency of radiation-induced mutants of blood cells is measured using flow cytometry. The TCR test is a cumulative biodosimeter, which measures the total radiation dose within the last 5 to 10 years, whereas the result of the MN-Tf-Ret test reflects the radiation dose of approximately 24 hours interval. It takes 8 hours and 3 days to perform TCR and MN-Tf-Ret tests respectively.

Calibration curves based on radioiodine treated patients can be used for dose estimation in humans, if the radiation conditions correspond to those in RIT. This limits their applicability to low dose-rate β - and γ -irradiation and to doses per session not higher than about 0.5 Sv. If higher doses or dose-rates as well as the other types of ionizing radiation are involved, calibration curves in animals are indispensable. In the case MN-Tf-Ret test mouse models are established and may be used.

The TCR assay was performed in 72 thyroid cancer patients aged between 14 and 25. T-cell mutant frequency (Mf) reaches its maximum only after half a year following the RIT. Then it declines exponentially. This decline could be described by the 3 parameter single exponential decay function.

Based on this equation, the radiation dose could be calculated when the Mf and the time interval since exposure are known. Furthermore, the experimentally measured Mf value, which significantly exceeds the corresponding calculated Mf value would indicate an individual with higher radiosensitivity. However, among our patients there were none.

The reticulocytes micronuclei test (MN-Tf-Ret) was performed in 46 radioiodine treated patients [78]. When measuring the MN frequency (f(MN-Tf-Ret)) the measured cell fraction should be limited only to the youngest cohort of reticulocytes, because all the micronucleated erythrocytes are quickly removed from the peripheral blood by spleen. Thus, the MN test was performed only in CD71 positive (having transferrin receptor) reticulocytes. These reticulocytes just entered the peripheral blood flow from red marrow.

The MN frequency was measured before the therapy and then every day after the irradiation until day 7. MN frequency curve has typical shape with latent period for days 0 to 3. Then there is a sharp increase in MN frequency which lasts for 24 hours and could start between days 3 and 4. In the following days the MN frequency is dropping to its base level that equals the one before the treatment. The decay of MN frequency is depending on the half-life of radioiodine in the patient organism. If the half-life is low, then the increased f(MN-Tf-Ret) lasts shorter and vice versa.

It was shown that the MN frequency curve could be described by the model where all the micronuclei arise only through the last mitosis of erythroblasts in the red marrow and the MN frequency is proportional to the radiation dose in the last cell cycle. The shape of this curve depends on the cell kinetics of erythropoiesis on one side and the exponential decay of radioiodine activity on the other. To the

best of our knowledge, the MN-Tf-Ret test was applied in the present study for the first time in biological dosimetry.

5. References

- [1] M.C. Mahoney, S. Lawvere, K.L. Falkner, Y.I. Averkin, V.A. Ostapenko, A.M. Michalek, K.B. Moysich, and P.L. McCarthy, *Thyroid cancer incidence trends in Belarus: examining the impact of Chernobyl*. Int J Epidemiol, 2004. **33**(5): p. 1025-33.
- [2] Y. Nikiforov, D.R. Gnepp, and J.A. Fagin, *Thyroid lesions in children and adolescents after the Chernobyl disaster: implications for the study of radiation tumorigenesis*. J Clin Endocrinol Metab, 1996. **81**(1): p. 9-14.
- [3] F. Pacini, T. Vorontsova, E.P. Demidchik, E. Molinaro, L. Agate, C. Romei, E. Shavrova, E.D. Cherstvoy, Y. Ivashkevitch, E. Kuchinskaya, M. Schlumberger, G. Ronga, M. Filesi, and A. Pinchera, *Post-Chernobyl thyroid carcinoma in Belarus children and adolescents: comparison with naturally occurring thyroid carcinoma in Italy and France*. J Clin Endocrinol Metab, 1997. **82**(11): p. 3563-9.
- [4] K.B. Moysich, R.J. Menezes, and A.M. Michalek, *Chernobyl-related ionising radiation exposure and cancer risk: an epidemiological review*. Lancet Oncol, 2002. **3**(5): p. 269-79.
- [5] C. Reiners and J. Farahati, *¹³¹I therapy of thyroid cancer patients*. Q J Nucl Med, 1999. **43**(4): p. 324-35.
- [6] S. Kyoizumi, S. Umeki, M. Akiyama, Y. Hirai, Y. Kusunoki, N. Nakamura, K. Endoh, J. Konishi, M.S. Sasaki, T. Mori, and et al., *Frequency of mutant T lymphocytes defective in the expression of the T-cell antigen receptor gene among radiation-exposed people*. Mutat Res, 1992. **265**(2): p. 173-80.
- [7] M. Akiyama, S. Umeki, Y. Kusunoki, S. Kyoizumi, N. Nakamura, T. Mori, Y. Ishikawa, M. Yamakido, K. Ohama, T. Kodama, and et al., *Somatic-cell mutations as a possible predictor of cancer risk*. Health Phys, 1995. **68**(5): p. 643-9.
- [8] A.S. Saenko, I.A. Zamulaeva, S.G. Smirnova, N.V. Orlova, E.I. Selivanova, V.A. Saenko, N.P. Matveeva, M.A. Kaplan, V.Y. Nugis, N.M. Nadezhina, and A.F. Tsyb, *Determination of somatic mutant frequencies at glycoporphin A and T-cell receptor loci for biodosimetry of prolonged irradiation*. Int J Radiat Biol, 1998. **73**(6): p. 613-8.

- [9] K. Hempel, *Genmutation als Marker für ein biologisches Monitoring*. Arbeitsmed. Sozialmed. Umweltmed., 2000. **35**: p. 577-592.
- [10] S. Kyoizumi, M. Akiyama, J.B. Cologne, K. Tanabe, N. Nakamura, A.A. Awa, Y. Hirai, Y. Kusunoki, and S. Umeki, *Somatic cell mutations at the glycophorin A locus in erythrocytes of atomic bomb survivors: implications for radiation carcinogenesis*. Radiat Res, 1996. **146**(1): p. 43-52.
- [11] N. Mei, N. Kunugita, S. Nomoto, and T. Norimura, *Comparison of the frequency of T-cell receptor mutants and thioguanine resistance induced by X-rays and ethylnitrosourea in cultured human blood T-lymphocytes*. Mutat Res, 1996. **357**(1-2): p. 191-7.
- [12] K.H. Mavournin, D.H. Blakey, M.C. Cimino, M.F. Salamone, and J.A. Heddle, *The in vivo micronucleus assay in mammalian bone marrow and peripheral blood. A report of the U.S. Environmental Protection Agency Gene-Tox Program*. Mutat Res, 1990. **239**(1): p. 29-80.
- [13] L. Abramsson-Zetterberg, G. Zetterberg, M. Bergqvist, and J. Grawe, *Human cytogenetic biomonitoring using flow-cytometric analysis of micronuclei in transferrin-positive immature peripheral blood reticulocytes*. Environ Mol Mutagen, 2000. **36**(1): p. 22-31.
- [14] S. Kyoizumi, M. Akiyama, Y. Hirai, Y. Kusunoki, K. Tanabe, and S. Umeki, *Spontaneous loss and alteration of antigen receptor expression in mature CD4+ T cells*. J Exp Med, 1990. **171**(6): p. 1981-99.
- [15] S.M. Hou, F.J. Van Dam, F. de Zwart, C. Warnock, M. Mognato, J. Turner, N. Podlutskaja, A. Podlutsky, R. Becker, Y. Barnett, C.R. Barnett, L. Celotti, M. Davies, E. Huttner, B. Lambert, and A.D. Tates, *Validation of the human T-lymphocyte cloning assay--ring test report from the EU concerted action on HPRT mutation (EUCAHM)*. Mutat Res, 1999. **431**(2): p. 211-21.
- [16] *Radiation Dose to Patients from Radiopharmaceuticals*, in *ICRP (International commission on Radiological Protection)*. 1988, Pergamon Press: Oxford. p. 275.
- [17] K. Hempel, J. Biko, R. Lorenz, and C. Reiners (unpublished results).

- [18] M.G. Stabin, *MIRDose: personal computer software for internal dose assessment in nuclear medicine*. J Nucl Med, 1996. **37**(3): p. 538-46.
- [19] M.G. Stabin, J.A. Siegel, R.B. Sparks, K.F. Eckerman, and H.B. Breitz, *Contribution to red marrow absorbed dose from total body activity: a correction to the MIRD method*. J Nucl Med, 2001. **42**(3): p. 492-8.
- [20] J.A. Siegel, D. Yeldell, D.M. Goldenberg, M.G. Stabin, R.B. Sparks, R.M. Sharkey, A. Brenner, and R.D. Blumenthal, *Red marrow radiation dose adjustment using plasma FLT3-L cytokine levels: improved correlations between hematologic toxicity and bone marrow dose for radioimmunotherapy patients*. J Nucl Med, 2003. **44**(1): p. 67-76.
- [21] L. Schelper, M. Lassmann, H. Hänscheid, J. Biko, and C. Reiners, *A method for retrospective estimating the dose to bone marrow after radioiodine therapy of children and young adults*, in *Radioaktivität in Mensch und Umwelt*. 1998, TÜV-Verlag: Köln. p. 81-85.
- [22] S.R. Thomas, R.C. Samarasinghe, M. Sperling, and H.R. Maxon, 3rd, *Predictive estimate of blood dose from external counting data preceding radioiodine therapy for thyroid cancer*. Nucl Med Biol, 1993. **20**(2): p. 157-62.
- [23] J.A. Retzlaff, W.N. Tauxe, J.M. Kiely, and C.F. Stroebel, *Erythrocyte volume, plasma volume, and lean body mass in adult men and women*. Blood, 1969. **33**(5): p. 649-61.
- [24] C.R. Becker, M. Schätzl, H. Feist, A. Bäuml, U.J. Schöpf, and M.F. Reiser, *Strahlenexposition bei der CT-Untersuchung des Thorax und Abdomens. Vergleich von Einzelschicht-, Spiral- und Elektronenstrahl-Computer-Tomographie*. Radiologie, 1998. **38**: p. 725-729.
- [25] M. Cristy, *Active bone marrow distribution as a function of age in humans*. Phys Med Biol, 1981. **26**(3): p. 389-400.
- [26] H.H. Günter, D. Junker, O. Schober, and H. Hundeshagen, *Dosimetrie des hämatopoetischen Systems bei der Radioiodtherapie des Schilddrüsenkarzinoms*. Strahlentherapie und Onkologie, 1987. **44**: p. 185-191.

- [27] E.M. Kaptein, H. Levenson, M.E. Siegel, M. Gadallah, and M. Akmal, *Radioiodine dosimetry in patients with end-stage renal disease receiving continuous ambulatory peritoneal dialysis therapy*. J Clin Endocrinol Metab, 2000. **85**(9): p. 3058-64.
- [28] M. Akiyama, S. Kyoizumi, Y. Hirai, Y. Kusunoki, K.S. Iwamoto, and N. Nakamura, *Mutation frequency in human blood cells increases with age*. Mutat Res, 1995. **338**(1-6): p. 141-9.
- [29] S. Umeki, Y. Kusunoki, J.B. Cologne, K.S. Iwamoto, Y. Hirai, T. Seyama, K. Ohama, and S. Kyoizumi, *Lifespan of human memory T-cells in the absence of T-cell receptor expression*. Immunol Lett, 1998. **62**(2): p. 99-104.
- [30] A.R. McLean and C.A. Michie, *In vivo estimates of division and death rates of human T lymphocytes*. Proc Natl Acad Sci U S A, 1995. **92**(9): p. 3707-11.
- [31] N. Ishioka, S. Umeki, Y. Hirai, M. Akiyama, T. Kodama, K. Ohama, and S. Kyoizumi, *Stimulated rapid expression in vitro for early detection of in vivo T-cell receptor mutations induced by radiation exposure*. Mutat Res, 1997. **390**(3): p. 269-82.
- [32] T. Papayannopoulou and C.A. Finch, *Radioiron measurements in red cell maturation*. Blood Cells, 1975. **1**: p. 535-546.
- [33] K.O. Skarberg, R. Cea, and P. Reizenstein, *Cellularity and cell proliferation rates in human bone marrow. II. Studies on generation times and radiothymidine uptake of human red cell precursors*. Acta Med Scand, 1974. **195**(4): p. 301-6.
- [34] J.W. Choi and S.H. Pai, *Reticulocyte subpopulations and reticulocyte maturity index (RMI) rise as body iron status falls*. Am J Hematol, 2001. **67**(2): p. 130-5.
- [35] S.H. Song and A.C. Groom, *Sequestration and possible maturation of reticulocytes in the normal spleen*. Can J Physiol Pharmacol, 1972. **50**(5): p. 400-6.
- [36] G. Kent, O.T. Minick, F.I. Volini, and E. Orfei, *Autophagic vacuoles in human red cells*. Am J Pathol, 1966. **48**(5): p. 831-57.

- [37] B. Hogstedt, B. Gullberg, E. Mark-Vendel, F. Mitelman, and S. Skerfving, *Micronuclei and chromosome aberrations in bone marrow cells and lymphocytes of humans exposed mainly to petroleum vapors*. *Hereditas*, 1981. **94**(2): p. 179-87.
- [38] S.D. Dertinger, Y. Chen, R.K. Miller, K.J. Brewer, T. Smudzin, D.K. Torous, N.E. Hall, K.A. Olvany, F.G. Murante, and C.R. Tometsko, *Micronucleated CD71-positive reticulocytes: a blood-based endpoint of cytogenetic damage in humans*. *Mutat Res*, 2003. **542**(1-2): p. 77-87.
- [39] M. Hayashi, T. Sofuni, and M. Ishidate, Jr., *Kinetics of micronucleus formation in relation to chromosomal aberrations in mouse bone marrow*. *Mutat Res*, 1984. **127**(2): p. 129-37.
- [40] F. Ludwikow and G. Ludwikow, *A two-compartment model of micronucleus formation in erythrocytes and its application to mouse bone marrow. I. Rectangularly transient action of clastogen in stationary conditions*. *J Theor Biol*, 1993. **165**(3): p. 417-28.
- [41] in *Hematology*, WS Beck, Editor. 1977, MIT Press Cambridge: Massachusetts. p. 17.
- [42] S. Angelini, R. Kumar, F. Carbone, F. Maffei, G.C. Forti, F.S. Violante, V. Lodi, S. Curti, K. Hemminki, and P. Hrelia, *Micronuclei in humans induced by exposure to low level of ionizing radiation: influence of polymorphisms in DNA repair genes*. *Mutat Res*, 2005. **570**(1): p. 105-17.
- [43] J.C. Hando, J. Nath, and J.D. Tucker, *Sex chromosomes, micronuclei and aging in women*. *Chromosoma*, 1994. **103**(3): p. 186-92.
- [44] G. Joksic, S. Petrovic, and Z. Ilic, *Age-related changes in radiation-induced micronuclei among healthy adults*. *Braz J Med Biol Res*, 2004. **37**(8): p. 1111-7.
- [45] L. Abramsson-Zetterberg, G. Zetterberg, and J. Grawe, *The time-course of micronucleated polychromatic erythrocytes in mouse bone marrow and peripheral blood*. *Mutat Res*, 1996. **350**(2): p. 349-58.
- [46] J.T. MacGregor, C.M. Wehr, and D.H. Gould, *Clastogen-induced micronuclei in peripheral blood erythrocytes: the basis of an improved micronucleus test*. *Environ Mutagen*, 1980. **2**(4): p. 509-14.

- [47] J. Grawe, L. Abramsson-Zetterberg, L. Eriksson, and G. Zetterberg, *The relationship between DNA content and centromere content in micronucleated mouse bone marrow erythrocytes analysed by flow cytometry and fluorescent in situ hybridization*. *Mutagenesis*, 1994. **9**(1): p. 31-8.
- [48] L. Abramsson-Zetterberg, J. Grawe, and G. Zetterberg, *Flow cytometric analysis of micronucleus induction in mice by internal exposure to ^{137}Cs at very low dose rates*. *Int J Radiat Biol*, 1995. **67**(1): p. 29-36.
- [49] R.C. Chaubey, H.N. Bhilwade, B.N. Joshi, and P.S. Chauhan, *Studies on the migration of micronucleated erythrocytes from bone marrow to the peripheral blood in irradiated Swiss mice*. *Int J Radiat Biol*, 1993. **63**(2): p. 239-45.
- [50] G.C. Jagetia and N.G. Ganapathi, *Radiation-induced micronucleus formation in mouse bone marrow after low dose exposures*. *Mutat Res*, 1994. **304**(2): p. 235-42.
- [51] D. Jenssen and C. Ramel, *Factors affecting the induction of micronuclei at low doses of X-rays, MMS and dimethylnitrosamine in mouse erythroblasts*. *Mutat Res*, 1978. **58**(1): p. 51-65.
- [52] P. Morales-Ramirez, T. Vallarino-Kelly, J. Mercader-Martinez, and R. Rodriguez-Reyes, *Induction of micronuclei by acute and chronic exposure in vivo to gamma rays in murine polychromatic erythrocytes*. *Mutat Res*, 1994. **341**(1): p. 47-55.
- [53] J. Grawe, G. Zetterberg, and H. Amneus, *Flow-cytometric enumeration of micronucleated polychromatic erythrocytes in mouse peripheral blood*. *Cytometry*, 1992. **13**(7): p. 750-8.
- [54] M. Lenarczyk, S.M. Goddu, D.V. Rao, and R.W. Howell, *Biologic dosimetry of bone marrow: induction of micronuclei in reticulocytes after exposure to ^{32}P and ^{90}Y* . *J Nucl Med*, 2001. **42**(1): p. 162-9.
- [55] M. Bauchinger, *Health impacts of large releases of radionuclides. Cytogenetic effects as quantitative indicators of radiation exposure*. *Ciba Found Symp*, 1997. **203**: p. 188-99; discussion 199-204, 232-4.

- [56] H. Stopper, K. Hempel, C. Reiners, S. Vershenya, R. Lorenz, V. Vukicevic, A. Heidland, and J. Grawe, *Pilot study for comparison of reticulocyte-micronuclei with lymphocyte-micronuclei in human biomonitoring*. *Toxicol Lett*, 2005. **156**(3): p. 351-60.
- [57] C. Streffer, W.U. Muller, A. Kryscio, and W. Bocker, *Micronuclei-biological indicator for retrospective dosimetry after exposure to ionizing radiation*. *Mutat Res*, 1998. **404**(1-2): p. 101-5.
- [58] M. De Boeck, B.J. van der Leede, F. Van Goethem, A. De Smedt, M. Steemans, A. Lampo, and P. Vanparys, *Flow cytometric analysis of micronucleated reticulocytes: Time- and dose-dependent response of known mutagens in mice, using multiple blood sampling*. *Environ Mol Mutagen*, 2005. **46**(1): p. 30-42.
- [59] D.K. Torous, N.E. Hall, A.H. Illi-Love, M.S. Diehl, K. Cederbrant, K. Sandelin, I. Ponten, G. Bolcsfoldi, L.R. Ferguson, A. Pearson, J.B. Majeska, J.P. Tarca, G.M. Hynes, A.M. Lynch, J.P. McNamee, P.V. Bellier, M. Parenteau, D. Blakey, J. Bayley, B.J. van der Leede, P. Vanparys, P.R. Harbach, S. Zhao, A.L. Filipunas, C.W. Johnson, C.R. Tometsko, and S.D. Dertinger, *Interlaboratory validation of a CD71-based flow cytometric method (Microflow) for the scoring of micronucleated reticulocytes in mouse peripheral blood*. *Environ Mol Mutagen*, 2005. **45**(1): p. 44-55.
- [60] S. Gutierrez, E. Carbonell, P. Galofre, A. Creus, and R. Marcos, *Cytogenetic damage after ¹³¹-iodine treatment for hyperthyroidism and thyroid cancer. A study using the micronucleus test*. *Eur J Nucl Med*, 1999. **26**(12): p. 1589-96.
- [61] M. Ballardini, F. Gemignani, L. Bodei, G. Mariani, M. Ferdeghini, A.M. Rossi, L. Migliore, and R. Barale, *Formation of micronuclei and of clastogenic factor(s) in patients receiving therapeutic doses of iodine-131*. *Mutat Res*, 2002. **514**(1-2): p. 77-85.
- [62] C. Catena, D. Conti, G. Trenta, E. Righi, F. Breuer, F.F. Melacrinis, T. Montesano, G. Ventroni, and G. Ronga, *Micronucleus yield and colorimetric test as*

indicators of damage in patients' lymphocytes after ¹³¹I therapy. J Nucl Med, 2000. **41**(9): p. 1522-4.

[63] G.K. Livingston, A.E. Foster, and H.R. Elson, *Effect of in vivo exposure to iodine-131 on the frequency and persistence of micronuclei in human lymphocytes.* J Toxicol Environ Health, 1993. **40**(2-3): p. 367-75.

[64] W.U. Muller, S. Dietl, K. Wuttke, C. Reiners, J. Biko, E. Demidchik, and C. Streffer, *Micronucleus formation in lymphocytes of children from the vicinity of Chernobyl after (¹³¹I) therapy.* Radiat Environ Biophys, 2004. **43**(1): p. 7-13.

[65] N. Watanabe, H. Kanegane, S. Kinuya, N. Shuke, K. Yokoyama, H. Kato, G. Tomizawa, M. Shimizu, H. Funada, and H. Seto, *The radiotoxicity of ¹³¹I therapy of thyroid cancer: assessment by micronucleus assay of B lymphocytes.* J Nucl Med, 2004. **45**(4): p. 608-11.

[66] K. Wuttke, C. Streffer, W.U. Muller, C. Reiners, J. Biko, and E. Demidchik, *Micronuclei in lymphocytes of children from the vicinity of Chernobyl before and after ¹³¹I therapy for thyroid cancer.* Int J Radiat Biol, 1996. **69**(2): p. 259-68.

[67] L. Popova, V. Hadjidekova, T. Hadjieva, S. Agova, and I. Vasilev, *Cytokinesis-block micronucleus test in patients undergoing radioiodine therapy for differentiated thyroid carcinoma.* Hell J Nucl Med, 2005. **8**(1): p. 54-7.

[68] L. Baugnet-Mahieu, M. Lemaire, E.D. Leonard, A. Leonard, and G.B. Gerber, *Chromosome aberrations after treatment with radioactive iodine for thyroid cancer.* Radiat Res, 1994. **140**(3): p. 429-31.

[69] T. Erselcan, S. Sungu, S. Ozdemir, B. Turgut, D. Dogan, and O. Ozdemir, *Iodine-131 treatment and chromosomal damage: in vivo dose-effect relationship.* Eur J Nucl Med Mol Imaging, 2004. **31**(5): p. 676-84.

[70] S. Gundy, N. Katz, M. Fuzy, and O. Esik, *Cytogenetic study of radiation burden in thyroid disease patients treated with external irradiation or radioiodine.* Mutat Res, 1996. **360**(2): p. 107-13.

[71] L. Lehmann, H. Zitzelsberger, A.M. Kellerer, H. Braselmann, U. Kulka, V. Georgiadou-Schumacher, T. Negele, F. Spelsberg, E. Demidchik, E. Lengfelder, and M. Bauchinger, *Chromosome translocations in thyroid tissues from*

Belarussian children exposed to radioiodine from the Chernobyl accident, measured by FISH-painting. Int J Radiat Biol, 1996. **70**(5): p. 513-6.

[72] D.C. Lloyd, R.J. Purrott, G.W. Dolphin, P.W. Horton, K.E. Halnan, J.S. Scott, and G. Mair, *A comparison of physical and cytogenetic estimates of radiation dose in patients treated with iodine-131 for thyroid carcinoma.* Int J Radiat Biol Relat Stud Phys Chem Med, 1976. **30**(5): p. 473-85.

[73] R. M'Kacher, J.D. Legal, M. Schlumberger, B. Aubert, N. Beron-Gaillard, A. Gausson, and C. Parmentier, *Sequential biological dosimetry after a single treatment with iodine-131 for differentiated thyroid carcinoma.* J Nucl Med, 1997. **38**(3): p. 377-80.

[74] R. M'Kacher, J.D. Legal, M. Schlumberger, P. Voisin, B. Aubert, N. Gaillard, and C. Parmentier, *Biological dosimetry in patients treated with iodine-131 for differentiated thyroid carcinoma.* J Nucl Med, 1996. **37**(11): p. 1860-4.

[75] S. Puerto, R. Marcos, M.J. Ramirez, P. Galofre, A. Creus, and J. Surralles, *Equal induction and persistence of chromosome aberrations involving chromosomes 1, 4 and 10 in thyroid cancer patients treated with radioactive iodine.* Mutat Res, 2000. **469**(1): p. 147-58.

[76] K. Hempel, W. Deubel, R. Lorenz, and C. Reiners, *High gradient magnetic cell sorting and internal standardisation substantially improve the assay for somatic mutations at the glycophorin A (GPA) locus.* Mutat Res, 2003. **525**(1-2): p. 29-42.

[77] J. Schiwietz, R. Lorenz, M. Scheubeck, W. Borner, and K. Hempel, *Improved determination of variant erythrocytes at the glycophorin A (GPA) locus and variant frequency in patients treated with radioiodine for thyroid cancer.* Int J Radiat Biol, 1996. **70**(2): p. 131-43.

[78] J. Grawe, J. Biko, R. Lorenz, C. Reiners, H. Stopper, S. Vershenya, V. Vukicevic, and K. Hempel, *Evaluation of the reticulocyte micronucleus assay in patients treated with radioiodine for thyroid cancer.* Mutat Res, 2005. **583**(1): p. 12-25.

6. Abbreviations

BW - body weight

f(MN-Tf-Ret) - frequency of micronucleated transferrin positive reticulocytes

FBS - fetal bovine serum

FCS - fetal calf serum

GPA - glycophorin A

HPRT - hypoxanthine-guanine phosphoribosyl transferase

ICRP - International commission on Radiological Protection

Mf - mutant frequency

MIRD - Medical Internal Radiation Dose

MN - micronuclei

MN-PCE - micronucleated polychromatic erythrocytes

MN-Tf-Ret – micronucleated transferrin-positive reticulocytes

MPC – magnetic particle concentrator

PCE - polychromatic erythrocytes

RI - radioiodine

RIT – radioiodine treatment

RM – red marrow

RT – residence time

TB – total body

TCR – T-cell receptor

TCR-Mf – T-cell receptor mutants frequency

Tf-Ret – transferrin-positive reticulocytes

TSH - thyroid-stimulating hormone

Acknowledgements

Prof. Hempel for supervising me during my whole time in Nuclear Medicine, providing me with information and helping with any problems that might be encountered

Prof. Reiners for giving an opportunity to my make my MD in his Clinic and being a my mentor all this time

Prof. Grawe for his time and patience during my training in his laboratory

Dr. Koutsampelas, Dr. Biko and Dr. Felbinger for their help with obtaining of the blood samples

Dr. Hänscheid for the careful review of the dosimetry chapter

Prof. Sebald for providing recombinant IL2 for cell culture experiments

Dr. Thomas for the help in cells irradiation experiments

Tanja Ruetzel for doing the lab work and being my companion during all this time

Curriculum Vitae

I was born on the 28th of August 1980 in Minsk, Belarus

From 1986 till 1994 I studied in the Secondary school #127 in Minsk, Belarus.

From 1994 till 1996 – in Belarusian State University Lyceum.

Starting in 1996 I was full-time student of Belarussian State Medical University and in 2002 successfully graduated with the major - general practitioner.

Since October 2002 till September 2004 I did M.D. training in the Laboratory of Biological Dosimetry, Clinic of Nuclear Medicine, University of Würzburg, Germany under the head of prof. Chr. Reiners.

Since 2004 I am enrolled in the MD/PhD program of Würzburg University and working in the field of system biology.

Stanislav Vershenya